

## Electronic Supplementary Information

### Photochemical H<sub>2</sub> Evolution from Water Catalyzed by Dichloro(diphenylbipyridine)platinum(II) Derivative Tethered to Multiple Viologen Acceptors

Kyoji Kitamoto<sup>\*ab</sup> and Ken Sakai<sup>\*abc</sup>

<sup>a</sup>Department of Chemistry, Faculty of Science, Kyushu University,

<sup>b</sup>International Institute for Carbon Neutral Energy Research (WPI-I2CNER), Kyushu University,

<sup>c</sup>Center for Molecular Systems (CMS), Kyushu University, 744 Moto-oka Nishi-ku, Fukuoka 819-0395, Japan.

E-mail: kyo\_kitamoto@chem.kyushu-univ.jp, ksakai@chem.kyushu-univ.jp

## Experimental Section

### Materials.

1-Hydroxybenzotriazole hydrate (HOBt·H<sub>2</sub>O), N,N'-dicyclo-hexylcarbodiimide (DCC), and H-Asp(OBzl)-OBzl·HCl were purchased from Watanabe Chemical Industries. All other chemicals and solvents were purchased from Kanto Chemicals Co., Inc. and used without further purification. 4,4'-Bis(*p*-carboxyphenyl)-2,2'-bipyridine,<sup>S1</sup> 1-(2-aminoethyl)-1'-methyl-4,4'-bipyridinium hexafluorophosphate,<sup>S2</sup> *cis*-PtCl<sub>2</sub>(DMSO),<sup>S3</sup> and [PtCl<sub>2</sub>(bpyMV4)](PF<sub>6</sub>)<sub>8</sub>·4H<sub>2</sub>O<sup>S4</sup> were synthesized as previously described.

### Synthesis of 4,4'-bis{*p*-L-Asp(OBzl)-phenyl}-2,2'-bipyridine (dppyOBzl).

To a solution of 4,4'-bis(*p*-carboxyphenyl)-2,2'-bipyridine (0.29 g, 0.700 mmol) in thionyl chloride (20 mL) was added a drop of dry DMF followed by refluxing for 5 h with stirring. After the reaction mixture was cooled down to room temperature, thionyl chloride was removed under reduced pressure to give the chlorocarbonyl derivative. A solution of the chlorocarbonyl derivative in dry CH<sub>2</sub>Cl<sub>2</sub> (50 mL) was dropwisely added to a solution consisting of H-Asp(OBzl)-OBzl·HCl (0.69 g, 1.97 mmol), dry Et<sub>3</sub>N (1 mL), and dry CH<sub>2</sub>Cl<sub>2</sub> (50 mL), kept at 0 °C, followed by stirring of the solution at room temperature for 24 h. The reaction mixture was washed with an aqueous 5% NaHCO<sub>3</sub> solution (100 mL × 3), an aqueous 5% citric acid (100 mL × 3), and brine (100 mL). The organic phase was dried over Na<sub>2</sub>SO<sub>4</sub> followed by removal of the volatiles by evaporation to afford the product. The product was reprecipitated by adding hexane to a solution of the product in a minimum amount of CH<sub>2</sub>Cl<sub>2</sub>; a pale brown solid (yield: 0.69 g, 94.7 %). <sup>1</sup>H NMR (DMSO-d<sub>6</sub> / TMS, ppm): δ 9.22 (d, J = 7.6 Hz, 2H), 8.92 (d, J = 5.5 Hz, 2H), 8.85 (s, 2H), 8.10 (d, J = 5.5 Hz, 8H), 7.97 (dd, J = 4.8, 1.4 Hz, 2H), 7.49-7.36 (m, 20H), 5.23 (s, 4H), 5.18 (s, 4H), 5.05 (q, J = 7.6 Hz, 2H), 3.18-3.03 (m, 4H); Anal. calcd for C<sub>60</sub>H<sub>50</sub>N<sub>4</sub>O<sub>10</sub>·3H<sub>2</sub>O (1041.11): C, 69.22; H, 5.42; N, 5.38. Found: C, 69.18; H, 5.01; N, 5.17.

### Synthesis of 4,4'-bis(*p*-L-Asp-phenyl)-2,2'-bipyridine.

A solution of 4,4'-bis{*p*-L-Asp(OBzl)-phenyl}-2,2'-bipyridine (0.22 g, 0.211 mmol) in a CH<sub>2</sub>Cl<sub>2</sub>/MeOH mixture (1 : 1 v/v, 100 mL) was catalytically reduced in the presence of 10 % Pd on activated charcoal (ca. 0.1 g) under H<sub>2</sub> at atmospheric pressure for 24 h, followed by removal of the catalyst by filtration. The filtrate was evaporated under reduced pressure. The residue was dissolved in a minimum amount of methanol, followed by addition of CH<sub>2</sub>Cl<sub>2</sub> to give the product as a colorless solid (yield : 0.12 g, 83.6 %). <sup>1</sup>H NMR (DMSO-d<sub>6</sub> / TMS, ppm): δ 8.93 (d, J = 7.6 Hz, 2H), 8.85 (d, J = 5.5 Hz, 2H), 8.78 (s, 2H), 8.06-8.02 (m, 8H), 7.90 (dd, J = 4.8,

1.4 Hz, 2H), 4.80 (q,  $J = 6.2$  Hz, 2H), 2.90-2.73 (m, 4H); Anal. calcd for  $C_{32}H_{26}N_4O_{10} \cdot 3H_2O$  (680.62): C, 56.47; H, 4.74; N, 8.23. Found: C, 56.13; H, 4.61; N, 8.40.

#### Synthesis of **dpbpyMV4(PF<sub>6</sub>)<sub>8</sub>·6H<sub>2</sub>O**.

4,4'-Bis(*p*-L-Asp-phenyl)-2,2'-bipyridine (90 mg, 0.132 mmol) and 1-(2-aminoethyl)-1'-methyl-4,4'-bipyridinium hexafluorophosphate (0.333 g, 0.659 mmol) in dry DMF (10 mL) were stirred in the presence of HOBt·H<sub>2</sub>O (0.162 g, 1.06 mmol) and DCC (0.272 g, 1.32 mmol) at 30 °C for 24 h. After the reaction mixture was filtered for the removal of insoluble materials, the solvent was removed under reduced pressure. The residue was dissolved in a minimum amount of acetonitrile, followed by addition of a saturated acetonitrile solution of tetraethylammonium bromide to give **dpbpyMV4(Br)<sub>8</sub>** as a pale yellow solid. This was collected by filtration and was dissolved in a minimum amount of water, followed by addition of a saturated aqueous solution of NH<sub>4</sub>PF<sub>6</sub> to give the product as a pale red solid. This was recrystallized from water and dried in vacuo (yield : 251 mg, 70.9 %). <sup>1</sup>H NMR (CD<sub>3</sub>CN / TMS, ppm) : δ 8.90-8.82 (m, 22H), 8.41-8.34 (m, 16H), 8.07-7.89 (m, 8H), 7.75 (d,  $J = 7.6$  Hz, 2H), 7.13 (t,  $J = 6.2$ , 2H), 6.76 (d,  $J = 6.2$ , 2H), 4.73-4.62 (m, 10H), 4.41-4.35 (m, 12H), 3.81-3.67 (m, 8H), 2.75-2.60 (m, 4H); Anal. Calcd for  $C_{84}H_{86}F_{48}N_{16}O_6P_8 \cdot 6H_2O$  (2683.49): C, 37.60; H, 3.68; N, 8.35. Found : C, 37.50; H, 3.61; N, 8.33.

#### Synthesis of **[PtCl<sub>2</sub>(dpbpyMV4)](PF<sub>6</sub>)<sub>8</sub>·5H<sub>2</sub>O** and **[PtCl<sub>2</sub>(dpbpyMV4)]Cl<sub>8</sub>·16H<sub>2</sub>O**.

This was prepared by refluxing a solution of *cis*-PtCl<sub>2</sub>(DMSO)<sub>2</sub> (25 mg, 0.0568 mmol) and **dpbpyMV4(PF<sub>6</sub>)<sub>8</sub>·6H<sub>2</sub>O** (0.15 g, 0.0559 mmol) in methanol (15 mL) for 6 h. After cooling down to room temperature, the resulting yellow solid was collected by filtration. This was recrystallized from water and dried in vacuo. (yield: 101 mg, 60.7 %). <sup>1</sup>H NMR (CD<sub>3</sub>CN / TMS, ppm): δ 9.77 (d,  $J = 6.2$  Hz, 2H), 8.96-8.78 (m, 16H), 8.65 (d,  $J = 2.1$  Hz, 2H), 8.46-8.36 (m, 16H), 8.09-7.98 (m, 10H), 7.78 (d,  $J = 7.6$ , 2H), 7.15 (t,  $J = 6.2$ , 2H), 6.79 (t,  $J = 6.2$ , 2H), 4.72-4.62 (m, 10H), 4.41-4.37 (m, 12H), 3.83-3.72 (m, 8H), 2.79-2.68 (m, 4H); Anal. calcd for  $C_{84}H_{86}Cl_2F_{48}N_{16}O_6P_8Pt \cdot 5H_2O$  (2931.46): C, 34.42; H, 3.30; N, 7.64. Found: C, 34.37; H, 3.10; N, 7.48.

The yellow precipitate **[PtCl<sub>2</sub>(dpbpyMV4)]Cl<sub>8</sub>·16H<sub>2</sub>O** was ion exchanged to its Cl<sup>-</sup> form by dissolving it in acetonitrile and reprecipitating by adding a saturated acetonitrile solution of tetra(*n*-butyl)ammonium chloride. Anal. calcd for  $C_{84}H_{86}Cl_{10}N_{16}O_6Pt \cdot 16H_2O$  (2253.53): C, 44.77; H, 5.28; N, 9.94. Found: C, 45.04; H, 5.13; N, 9.59.

#### Synthesis of **PtCl<sub>2</sub>(dpbpyOBzl)·3H<sub>2</sub>O**.

This was prepared by refluxing a solution of *cis*-PtCl<sub>2</sub>(DMSO)<sub>2</sub> (41 mg, 0.0971 mmol) and

4,4'-bis{*p*-L-Asp(OBzl)-phenyl}-2,2'-bipyridine (0.10 g, 0.0961 mmol) in methanol (15 mL) for 6 h. After cooling down to room temperature, the resulting dark yellow solid was collected by filtration (yield: 90 mg, 70.9 %).  $^1\text{H}$  NMR ( $\text{CD}_3\text{CN}$  / TMS, ppm):  $\delta$  9.57 (d,  $J = 6.2$  Hz, 2H), 9.23 (d,  $J = 7.6$  Hz, 2H), 9.15 (s, 2H), 8.31 (dd,  $J = 6.2, 2.0$  Hz, 2H), 8.26 (d,  $J = 8.2$  Hz, 4H), 8.08 (d,  $J = 8.2$  Hz, 4H), 7.37-7.30 (m, 20H), 5.16-5.10 (m, 8H), 4.98 (q,  $J = 7.6$  Hz, 2H), 3.13-2.97 (m, 4H); Anal. calcd for  $\text{C}_{60}\text{H}_{50}\text{Cl}_2\text{N}_4\text{O}_{10}\text{Pt}\cdot 3\text{H}_2\text{O}$  (1307.07): C, 55.13; H, 4.32; N, 4.29. Found: C, 54.94; H, 3.88; N, 4.45.

### Measurements.

$^1\text{H}$  NMR spectra were acquired on a JEOL JNM-ESA 600 spectrometer. UV-vis and UV-vis-NIR spectra were recorded on Shimadzu UV-2600 and UV-3600 spectrophotometer, respectively. Low temperature emission spectra were measured for the glassy 77-K solution of each complex in a 4:4:1 (v/v/v) MeOH/EtOH/DMF mixture (abbreviated as MED, where DMF = dimethylformamide), contained in a quartz EPR tube. Emission decays were recorded on an HORIBA FluoroCube 3000USKU. The excitation source was a diode laser (374 nm) (HORIBA N-375L). Nanosecond laser flash photolysis experiments were carried out using a Unisoku TSP-1000M-03R system equipped with a Nd:YAG laser (Minilite II-10, Continuum, CA, USA) as a pump source and a 150 W Xe lamp (L2195, Hamamatsu) as a probe source. Nanosecond transient absorption spectra were recorded using multichannel detector with a gated image-intensifier (C954603, Hamamatsu), while single-wavelength transient absorption traces were monitored using an amplified photomultiplier tube (R2949, Hamamatsu). Cyclic voltammograms were recorded on a BAS ALS Model 6022D electrochemical analyser, using a three electrode system consisting of a platinum working electrode, a platinum wire counter electrode, and a  $\text{Ag}/\text{Ag}^+$  reference electrode (0.249 V vs. SCE), where TBAP (tetra(n-butyl)ammonium perchlorate) was used as a supporting electrolyte and all potentials reported were standardized by simultaneously observing the  $\text{Fc}/\text{Fc}^+$  couple ( $\text{Fc}/\text{Fc}^+ = 0.155$  V vs. SCE). Dynamic light scattering (DLS) data were measured using an Otsuka Electronics ELSZ-2PS particle analyzer equipped with a diode laser (660 nm) (detection limit : 0.6 nm in particle diameter).

### **Photochemical H<sub>2</sub> Evolution Experiments.**

Visible light irradiation ( $400 < \lambda < 800$  nm) was carried out using an ILC Technology CERMAX LX-300 Xe lamp (300 W) equipped with a CM-1 cold mirror which suppresses UV and NIR irradiation. Photolysis was carried out in a Pyrex glass vial (ca. 20 mL in inner volume), immersed in a water bath thermostatted at 20 °C, and each photolysis solution (10 mL) was continuously purged with Ar (10 mL/min; STEC SEC-E40/PAC-D2 digital mass flow controller) with stirring. The vent gas was introduced into our computer-controlled automated gas chromatographic analysis line (Shimadzu GC-8A gas chromatograph equipped with a molecular sieve 5A column (2 m x 3 mm i.d.; 30 °C) with an Ar carrier), the details for which have been described elsewhere.<sup>S5</sup>

### **Picosecond Transient Absorption Spectroscopy.**

Picosecond transient absorption spectroscopy was carried out using an ultrafast source; Solstice (Spectra Physics), and a commercially available ultrafast detection system, Helios (Ultrafast Systems LLC). The source for the pump and probe pulses were derived from the fundamental output of Solstice (800 nm, 2 mJ/pulse and fwhm = 130 fs) at a repetition rate of 1 kHz. In our experiments, 400-nm pump source, SHG light of the fundamental, was irradiated at the sample cell with a spot size of 1 mm diameter where it was merged with the white probe pulse in a close angle (<10 degree). The probe beam after passing through the 1 mm sample cell was focused on a fiber optic cable which was connected to a spectrograph with CMOS linear-array for recording the time-resolved spectra (435–850nm).

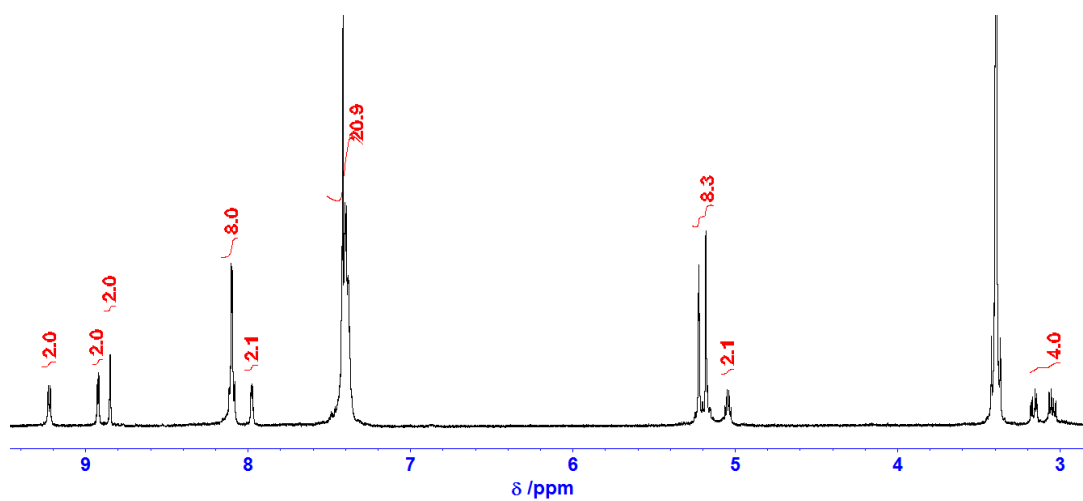


**Figure S1.**  $^1\text{H}$  NMR spectrum of 4,4'-bis{*p*-L-Asp(OBzl)-phenyl}-2,2'-bipyridine (dpbpyOBzl) in  $(\text{CD}_3)_2\text{SO}$  at room temperature.

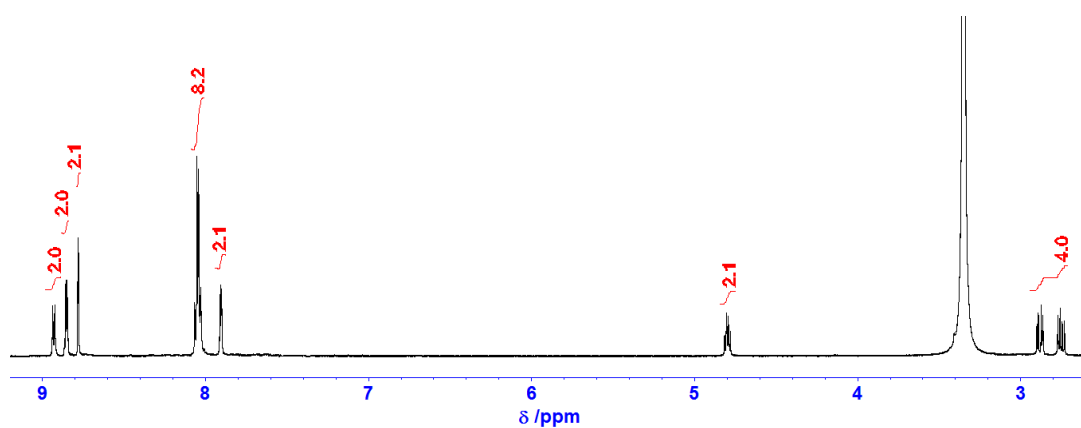


**Figure S2.**  $^1\text{H}$  NMR spectrum of 4,4'-bis(*p*-L-Asp-phenyl)-2,2'-bipyridine in  $(\text{CD}_3)_2\text{SO}$  at room temperature.

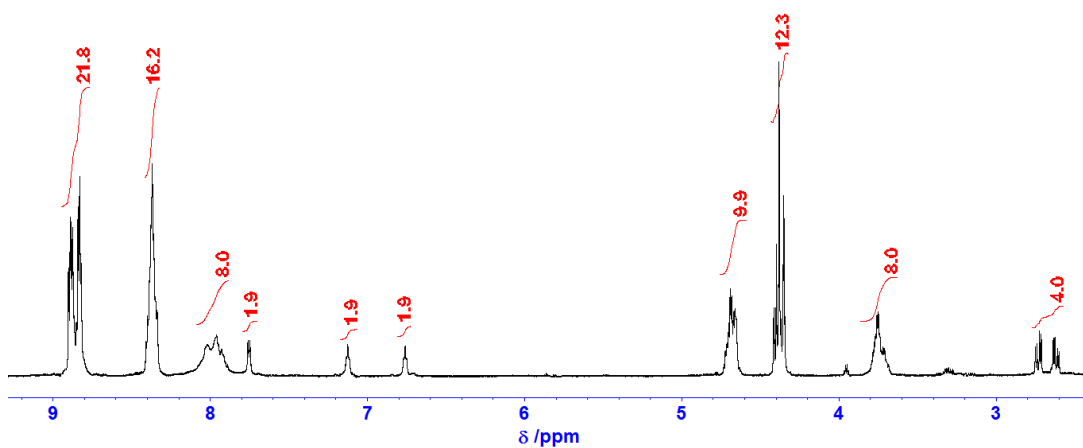


**Figure S3.**  $^1\text{H}$  NMR spectrum of dpbpyMV4( $\text{PF}_6$ ) $_8$  in  $\text{CD}_3\text{CN}$  at room temperature.

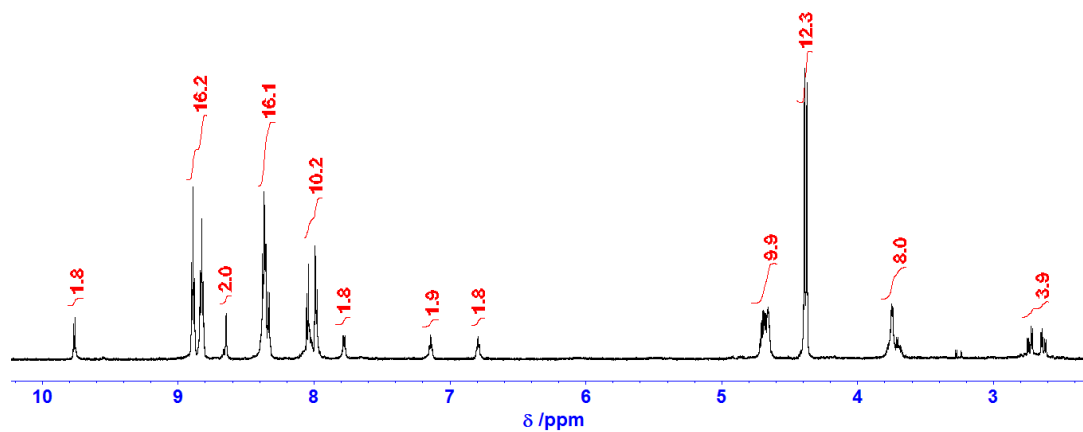


**Figure S4.**  $^1\text{H}$  NMR spectrum of  $[\text{PtCl}_2(\text{dpbpyMV4})](\text{PF}_6)_8$  in  $\text{CD}_3\text{CN}$  at room temperature.

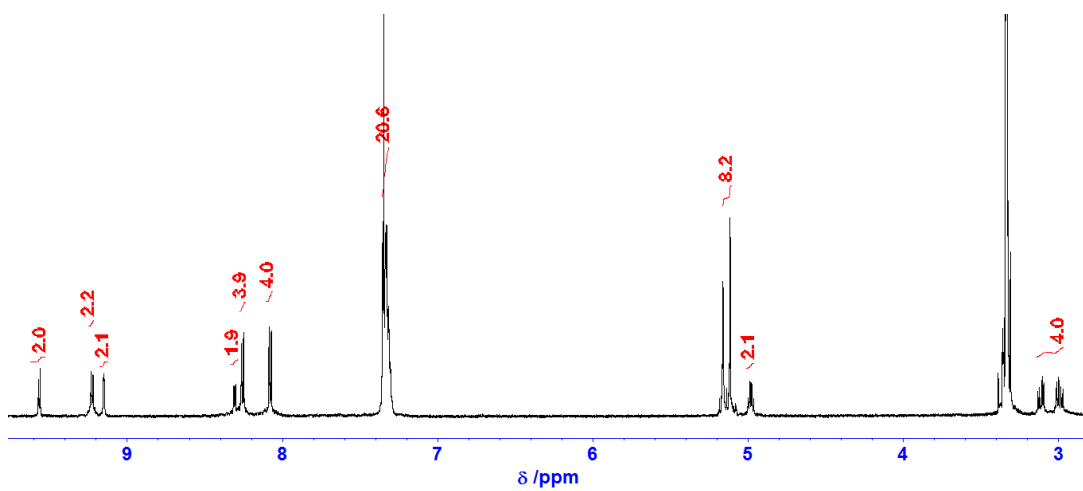


**Figure S5.**  $^1\text{H}$  NMR spectrum of  $\text{PtCl}_2(\text{dpbpyOBzl})$  in  $\text{CD}_3\text{CN}$  at room temperature.

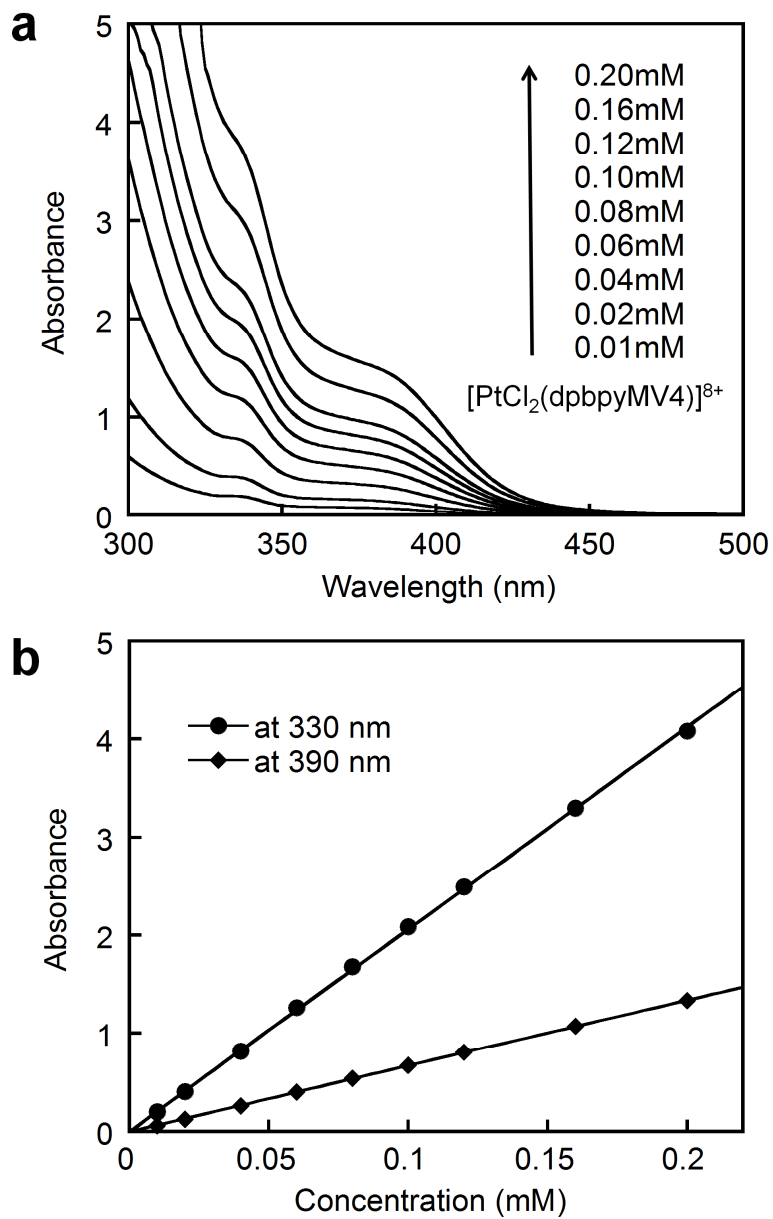


**Figure S6.** (a) UV-vis absorption spectra of  $[\text{PtCl}_2(\text{dpbyMV4})](\text{PF}_6)_8$  (**1**) in aqueous 0.1 M NaCl solution at various concentrations at 20 °C in air. (b) The concentration dependence of absorbance at two wavelengths in the concentration range of 0.01–0.2 mM, showing that **1** obeys the Beer's law.

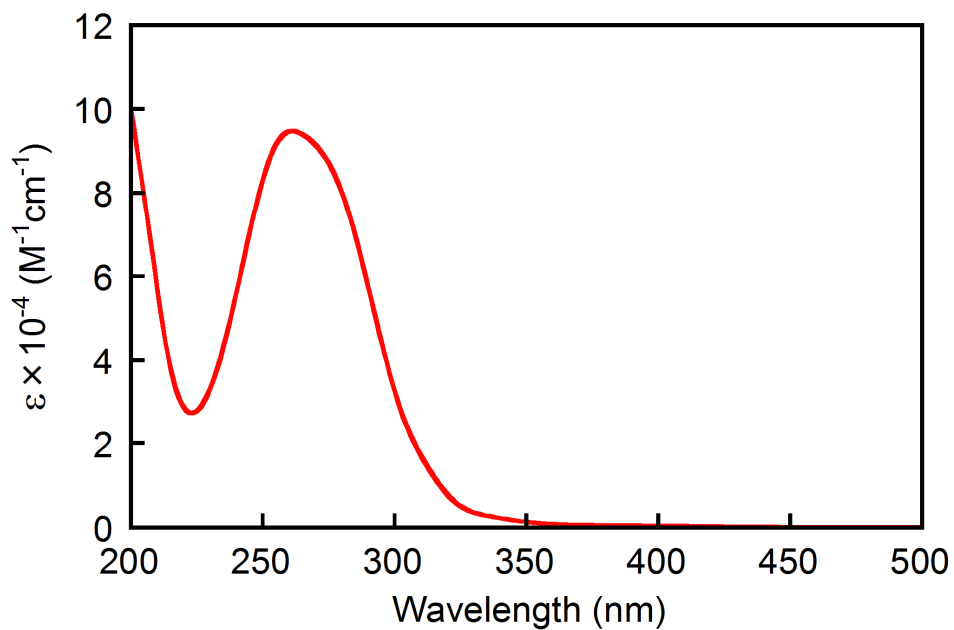


**Figure S7.** An absorption spectrum of  $\text{dpbpyMV4(PF}_6\text{)}_8$  in water at 20 °C in air.

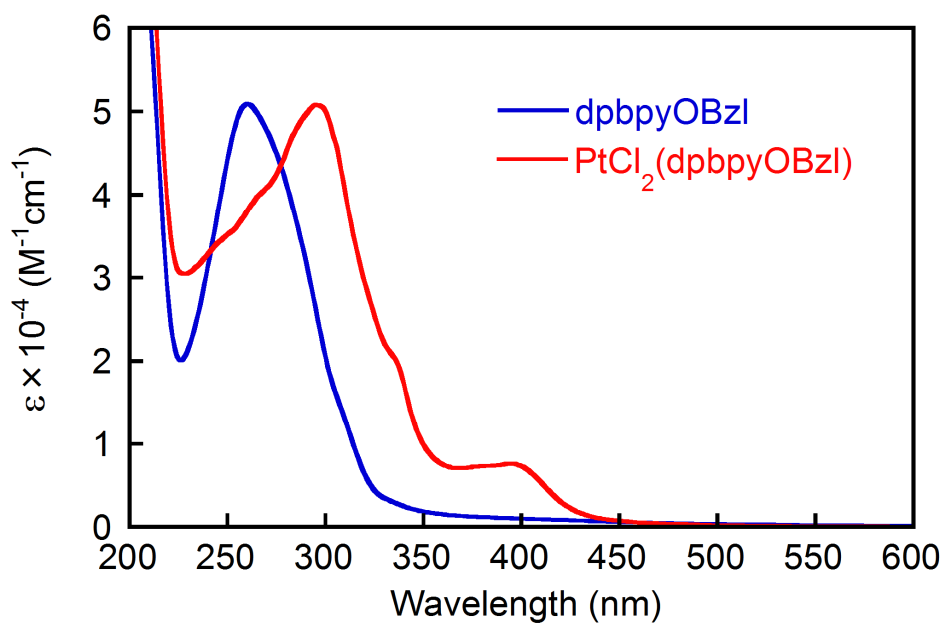


**Figure S8.** Absorption spectra of  $\text{dbbpyOBzl}$  and  $\text{PtCl}_2(\text{dpbpyOBzl})$  in acetonitrile at 20 °C in air.

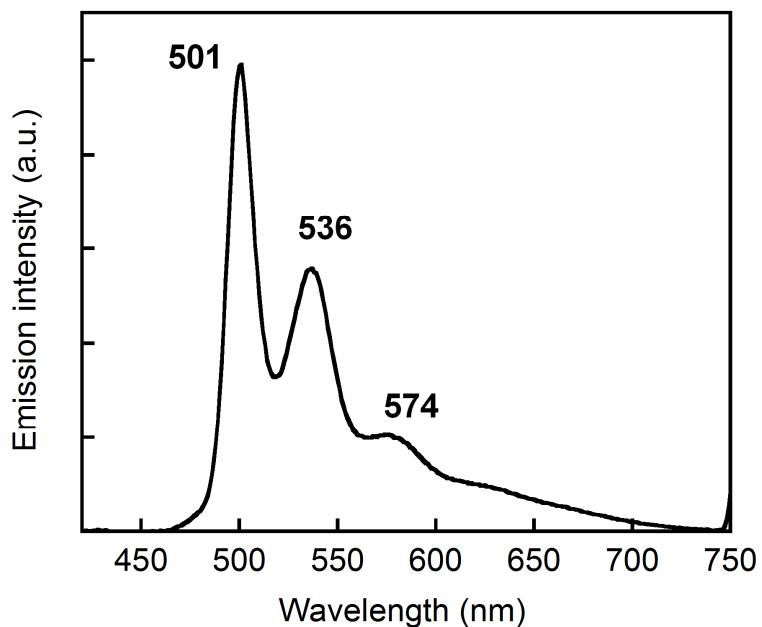


**Figure S9.** An emission spectrum of  $[\text{PtCl}_2(\text{dpbyMV4})](\text{PF}_6)_8$  in MED glass at 77 K (excitation at 380 nm).

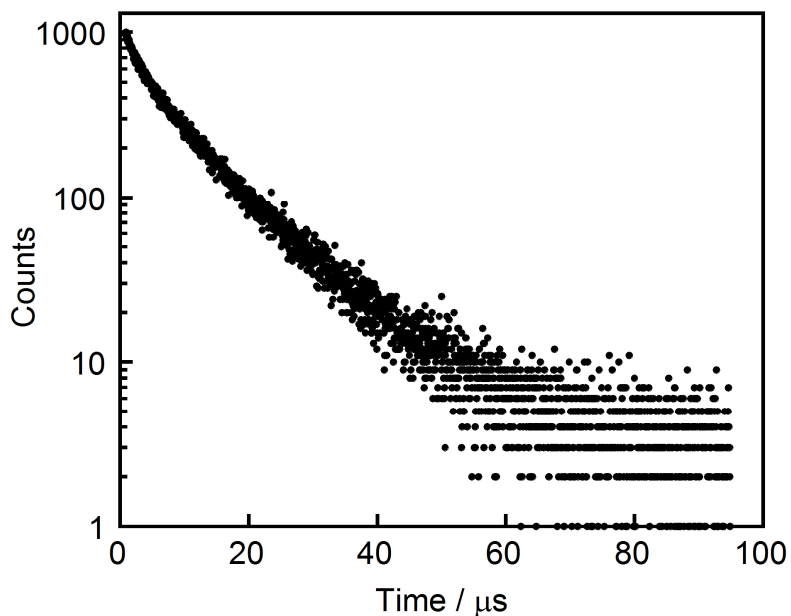


**Figure S10.** An emission decay profile of  $[\text{PtCl}_2(\text{dpbyMV4})](\text{PF}_6)_8$  in MED glass at 77 K. (excitation at 374 nm). The emission was monitored at 500 nm. The observed data could be fitted to a triple exponential function (see Table S1).

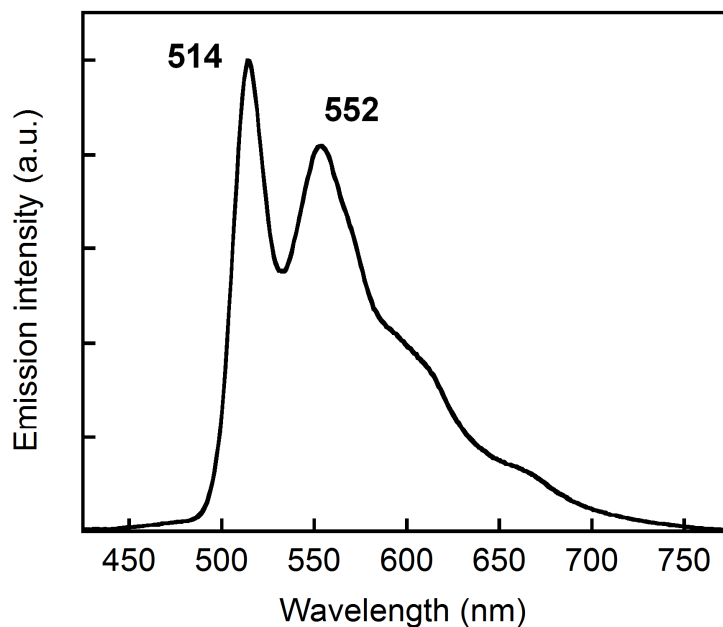


**Figure S11.** An emission spectrum of  $\text{PtCl}_2(\text{dpbbpyOBzl})$  in MED glass at 77 K (excitation at 400 nm).

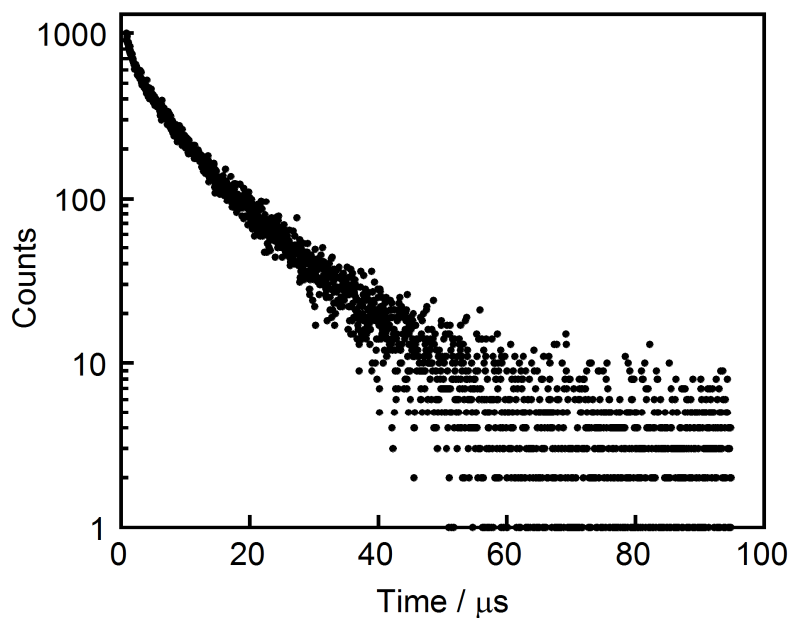


**Figure S12.** An emission decay profile of  $\text{PtCl}_2(\text{dpbbpyOBzl})$  in MED glass at 77 K. (excitation at 374 nm). The emission was monitored at 500 nm. The observed data could be fitted to a triple exponential function (see Table S1).

**Table S1.** Emission properties of relevant platinum complexes in MED glass at 77 K.

Complex	$\lambda_{\text{em}} / \text{nm}$	$\tau / \mu\text{s}$ (Relative contribution)
<b>[PtCl<sub>2</sub>(bpyMV4)](PF<sub>6</sub>)<sub>8</sub><sup>a</sup></b>	489, 527	9.13
<b>[PtCl<sub>2</sub>(dpbpyMV4)](PF<sub>6</sub>)<sub>8</sub></b>	501, 536, 574	1.38 (4.7 %) <sup>b</sup>
		6.06 (31.8 %)
		12.8 (63.5 %)
<b>PtCl<sub>2</sub>(dpbpyOBzl)</b>	514, 552	1.01 (2.4 %) <sup>b</sup>
		5.38 (28.4 %)
		12.3 (69.2 %)

<sup>a</sup>Values taken from ref. S4. <sup>b</sup>Lifetimes were estimated by fitting each decay at 500 nm to a triple exponential function.

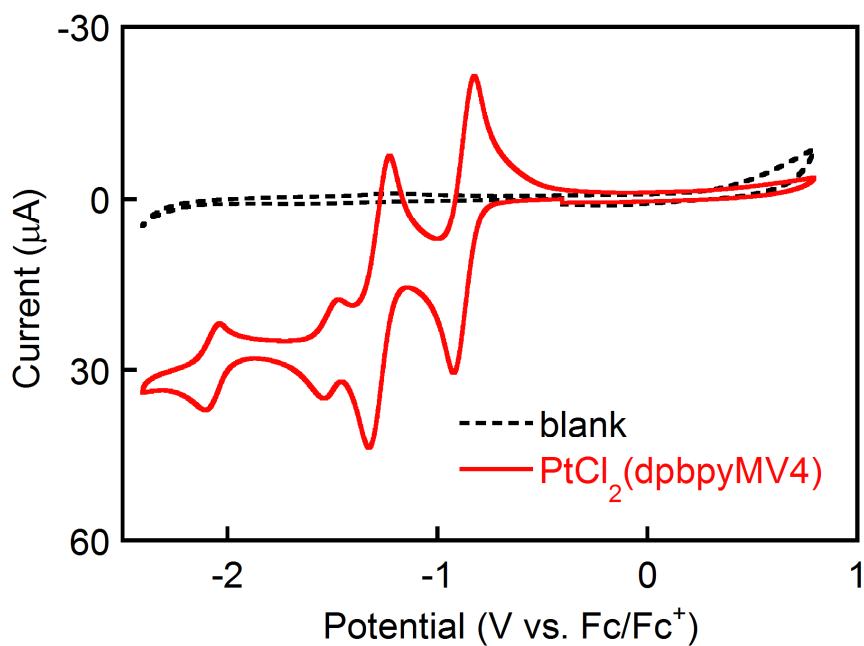


**Figure S13.** A cyclic voltammogram of  $[\text{PtCl}_2(\text{dpbbpyMV4})](\text{PF}_6)_8$  (1 mM) in a DMF solution containing 0.1 M TBAP at room temperature under Ar atmosphere, at a scan rate of  $100 \text{ mVs}^{-1}$ .

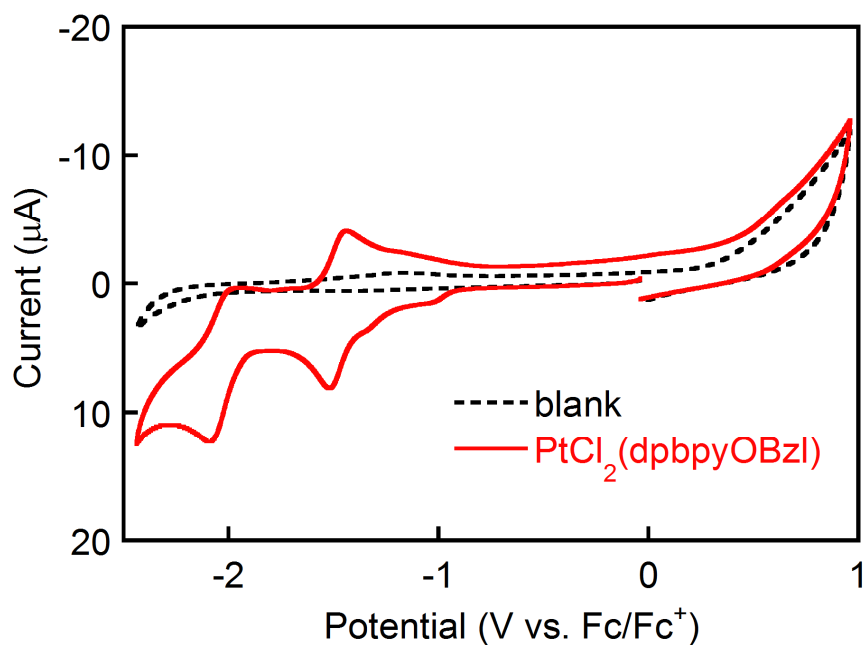


**Figure S14.** A cyclic voltammogram of  $\text{PtCl}_2(\text{dpbbpyOBzl})$  (1 mM) in a DMF solution containing 0.1 M TBAP at room temperature under Ar atmosphere, at a scan rate of  $100 \text{ mVs}^{-1}$ .

**Table S2.** Reduction potentials (V vs. Fc/Fc<sup>+</sup>) and  $\Delta G_{\text{IET}}$  for [PtCl<sub>2</sub>(bpyMV4)](PF<sub>6</sub>)<sub>8</sub> and [PtCl<sub>2</sub>(dpbpyMV4)](PF<sub>6</sub>)<sub>8</sub>, together with those for PtCl<sub>2</sub>(dpbpyOBzl).<sup>a</sup>

Compound	Redox potentials (V vs. Fc/Fc <sup>+</sup> )				$\Delta G_{\text{IET}}$ /eV
	$E_{1/2}$ (A/A <sup>-•</sup> )	$E_{1/2}$ (A <sup>-•</sup> /A <sup>2-</sup> )	$E_{1/2}$ (L/L <sup>-•</sup> )	$E_{1/2}$ (Pt <sup>III/I</sup> )	
[PtCl <sub>2</sub> (bpyMV4)](PF <sub>6</sub> ) <sub>8</sub> <sup>b</sup>	-0.81	-1.21	-1.35	-1.95	-0.54
[PtCl <sub>2</sub> (dpbpyMV4)](PF <sub>6</sub> ) <sub>8</sub>	-0.85	-1.25	-1.46	-2.03	-0.61
PtCl <sub>2</sub> (dpbpyOBzl)	--	--	-1.46	-2.01	--

<sup>a</sup>Measured in DMF using TBAP (0.1 M) as the supporting electrolyte. <sup>b</sup>Values taken from ref. S4.

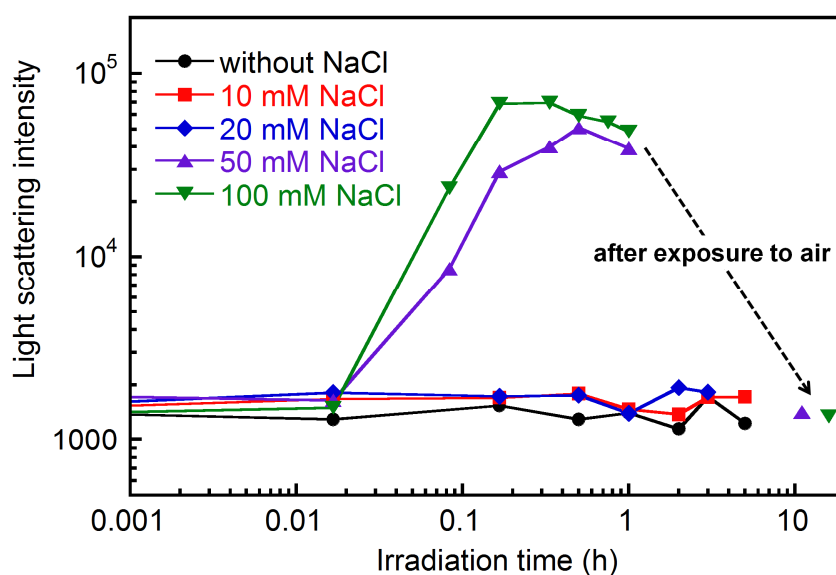


**Figure S15.** DLS measurements during the photolysis of an aqueous acetate buffer solution (0.03 M CH<sub>3</sub>COOH and 0.07 M CH<sub>3</sub>COONa; pH 5.0, at 20 °C under Ar) containing 30 mM EDTA and 0.05 mM [PtCl<sub>2</sub>(dpbpyMV4)]Cl<sub>8</sub> in the presence of NaCl at various concentrations.

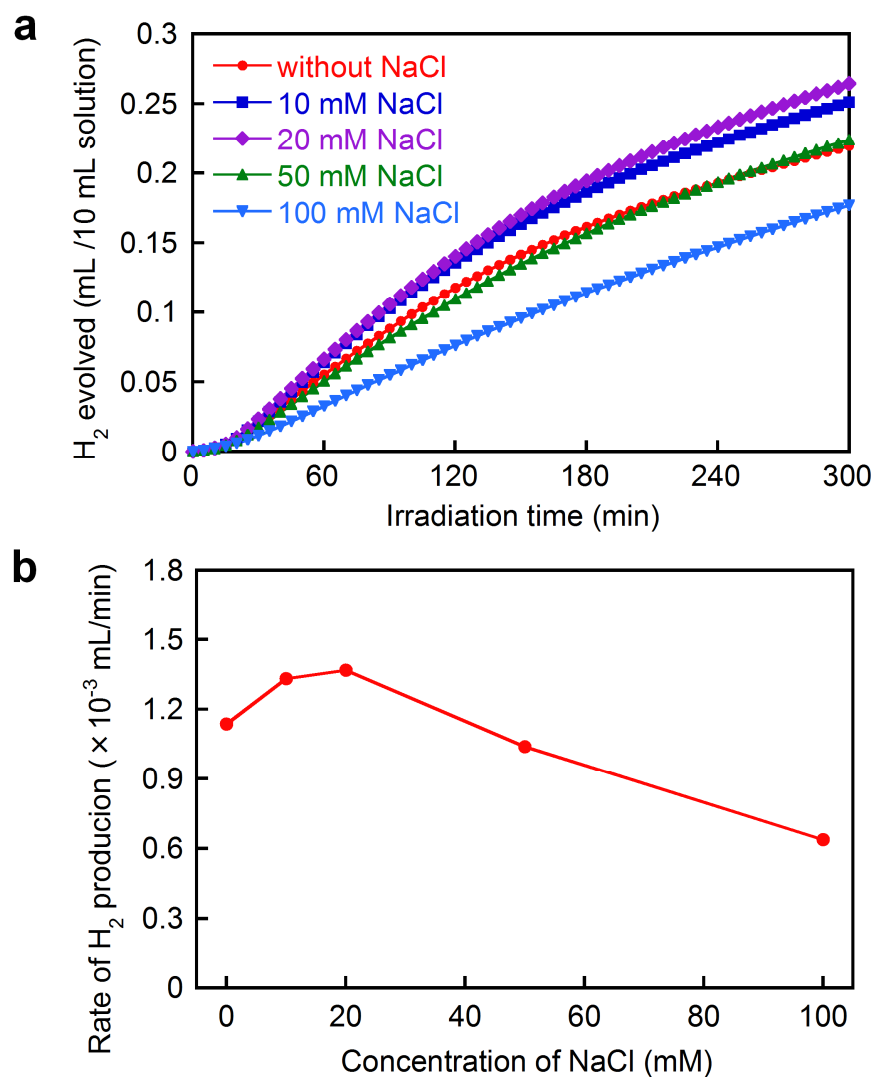


**Figure S16.** (a) Visible light-driven H<sub>2</sub> production (> 400 nm) from an aqueous acetate buffer solution (0.03 M CH<sub>3</sub>COOH and 0.07 M CH<sub>3</sub>COONa; pH 5.0, 10 mL, at 20 °C under Ar) containing 30 mM EDTA and 0.05 mM [PtCl<sub>2</sub>(dpbpyMV4)]Cl<sub>8</sub> (**1**) in the presence of NaCl at various concentrations. (b) The dependence of the initial rate of H<sub>2</sub> production on the NaCl concentration.

**Table S3.** Combinations of filters employed to select the wavelength regions in the photolysis experiments.<sup>a</sup>

Filters <sup>b</sup>	$\lambda^c$ (nm)	Range (nm)	Power <sup>d</sup> (W / cm <sup>2</sup> )	Photon flux <sup>e</sup> ( $\times 10^{-7}$ einstein/s)	
Pyrex glass + SU400	336	300–400	0.292	4.60	Fig. S17
SU400 + SV490	379	350–400	0.170	2.95	Fig. S18
L40 + SV450	421	390–450	0.231	4.56	Fig. S19
Y44 + SV490	462	430–490	0.177	3.83	Fig. S20
Y48 + DM-G	517	470–550	0.180	4.36	Fig. S21

<sup>a</sup>The photoirradiation was carried out by a ILC Technology CERMAX LX-300 Xe lamp (300 W) equipped with a CM-2 cold mirror ( $240 < \lambda < 550$  nm). <sup>b</sup>The interference filters employed are as follow: Pyrex glass ( $\lambda > 300$  nm), HOYA L40 ( $\lambda > 400$  nm), HOYA Y44 ( $\lambda > 440$  nm), HOYA Y48 ( $\lambda > 480$  nm), Asahi Spectra SU400 ( $200 < \lambda < 400$  nm), Asahi Spectra SV450 ( $350 < \lambda < 450$  nm), and Asahi Spectra SV490 ( $350 < \lambda < 490$  nm), HOYA DM-G ( $350 < \lambda < 550$  nm), where wavelengths correspond to those where the transmittance is 50 %. <sup>c</sup>The mean value for the wavelength of light. <sup>d</sup>The OPHIR Nova II power meter was used to determine the power of light irradiated. <sup>e</sup>The values were estimated from the mean  $\lambda$  values and the powers listed in this table, together with the results of chemical actinometry conducted for the set of SU400 and SV490.

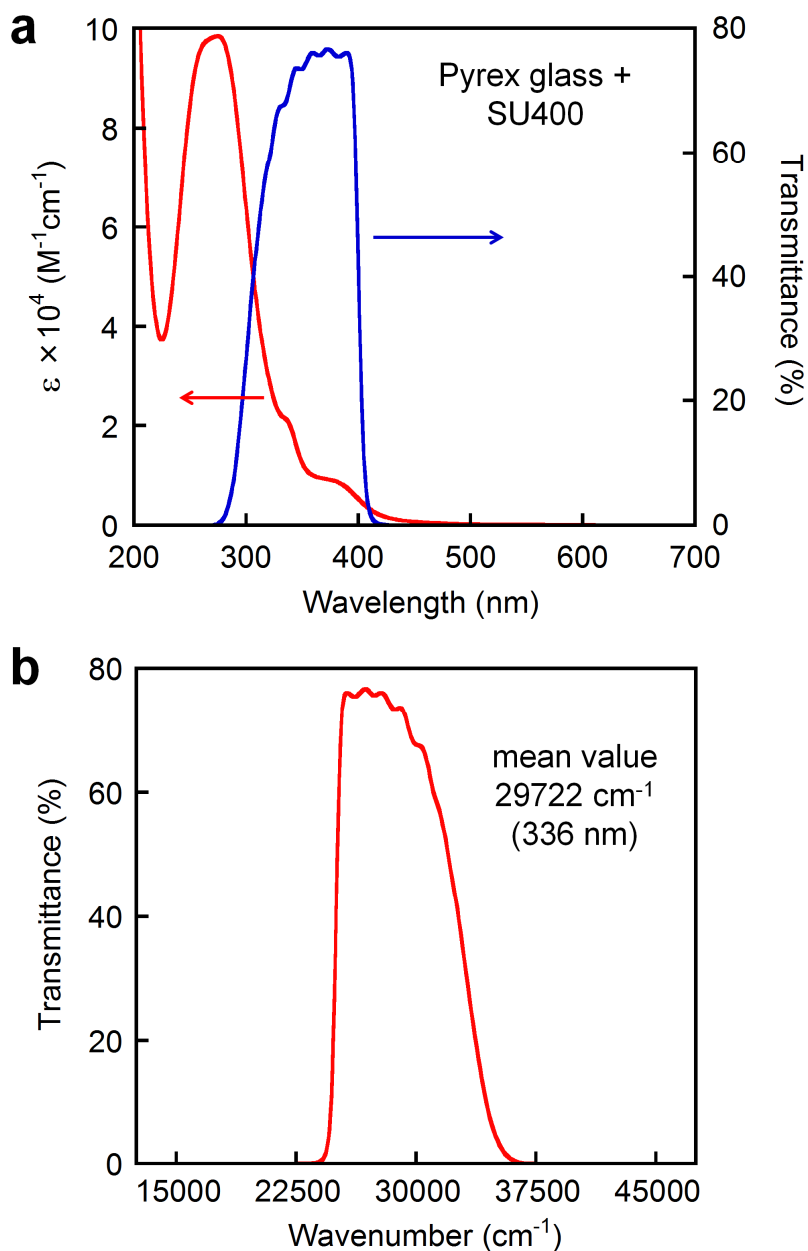


**Figure S17.** (a) Transmission spectrum for a set of interference filters Pyrex glass + SU400 (blue line), and the molar absorptivity ( $\epsilon$ ) spectrum of  $[\text{PtCl}_2(\text{dpbyMV4})](\text{PF}_6)_8$  in a 0.1 M NaCl aqueous solution at 20 °C in air (red line). (b) Transmission spectrum for a set of interference filters Pyrex glass + SU400 as a function of wavenumber, which was used to determine the mean value for the light energy.

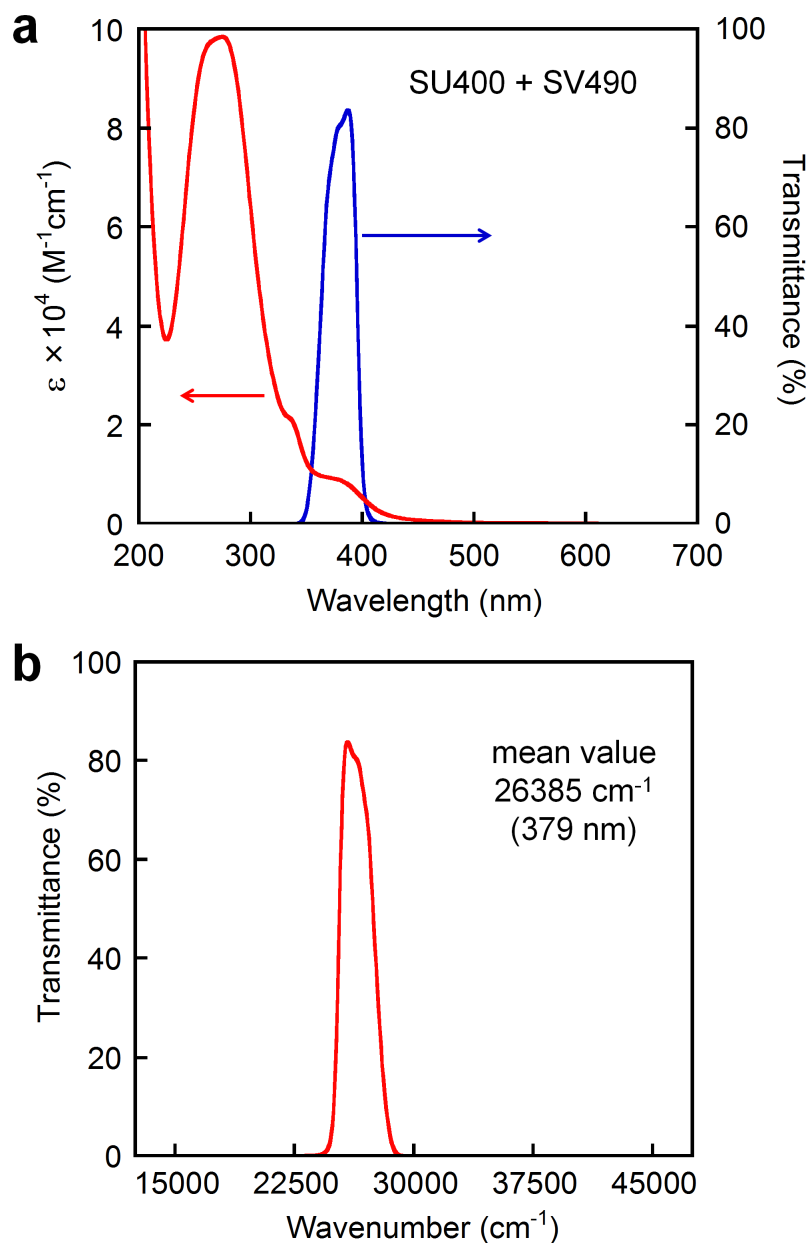


**Figure S18.** (a) Transmission spectrum for a set of interference filters SU400 + SV490 (blue line), and the molar absorptivity ( $\epsilon$ ) spectrum of  $[\text{PtCl}_2(\text{dpbyMV4})](\text{PF}_6)_8$  in a 0.1 M NaCl aqueous solution at 20 °C in air (red line). (b) Transmission spectrum for a set of interference filters SU400 + SV490 as a function of wavenumber, which was used to determine the mean value for the light energy.

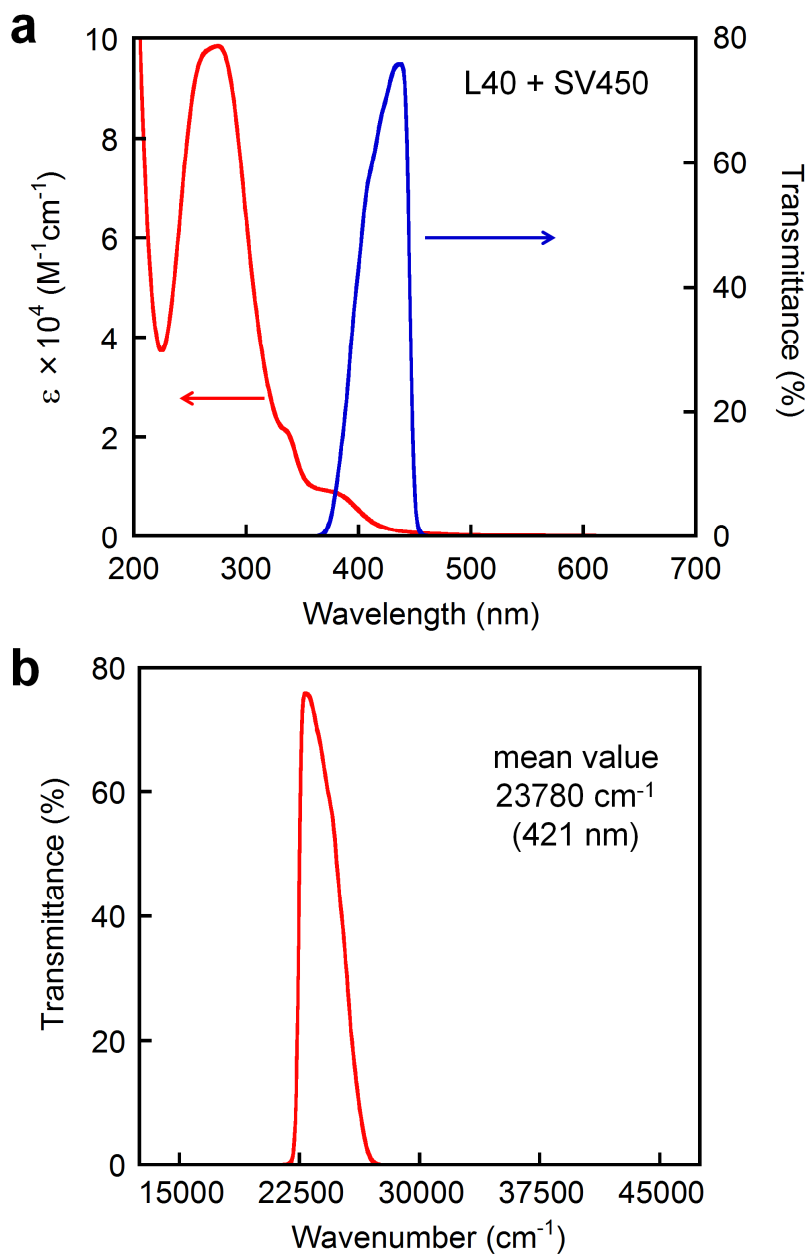


**Figure S19.** (a) Transmission spectrum for a set of interference filters L40 + SV450 (blue line), and the molar absorptivity ( $\epsilon$ ) spectrum of  $[\text{PtCl}_2(\text{dpbyMV4})](\text{PF}_6)_8$  in a 0.1 M NaCl aqueous solution at 20 °C in air (red line). (b) Transmission spectrum for a set of interference filters L40 + SV450 as a function of wavenumber, which was used to determine the mean value for the light energy.

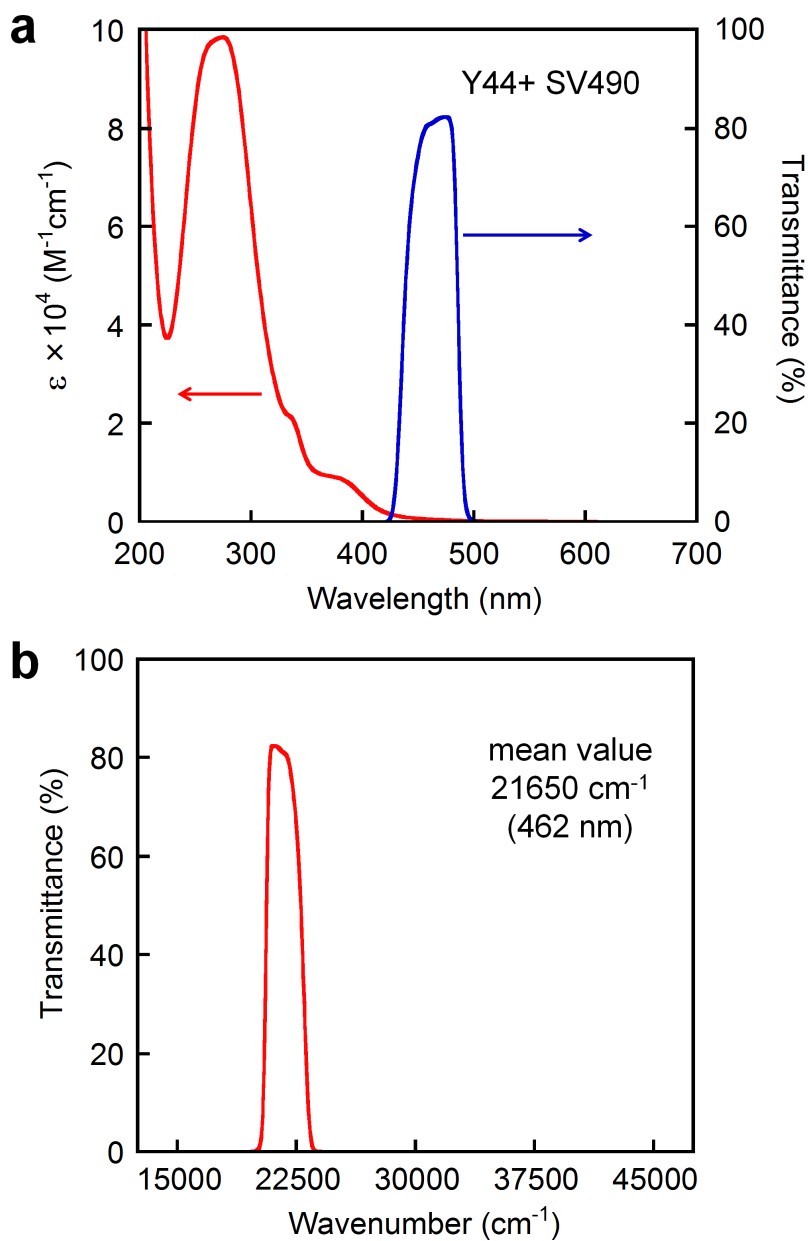


**Figure S20.** (a) Transmission spectrum for a set of interference filters Y44 + SV490 (blue line), and the molar absorptivity ( $\epsilon$ ) spectrum of  $[\text{PtCl}_2(\text{dpbpyMV4})](\text{PF}_6)_8$  in a 0.1 M NaCl aqueous solution at 20 °C in air (red line). (b) Transmission spectrum for a set of interference filters Y44 + SV490 as a function of wavenumber, which was used to determine the mean value for the light energy

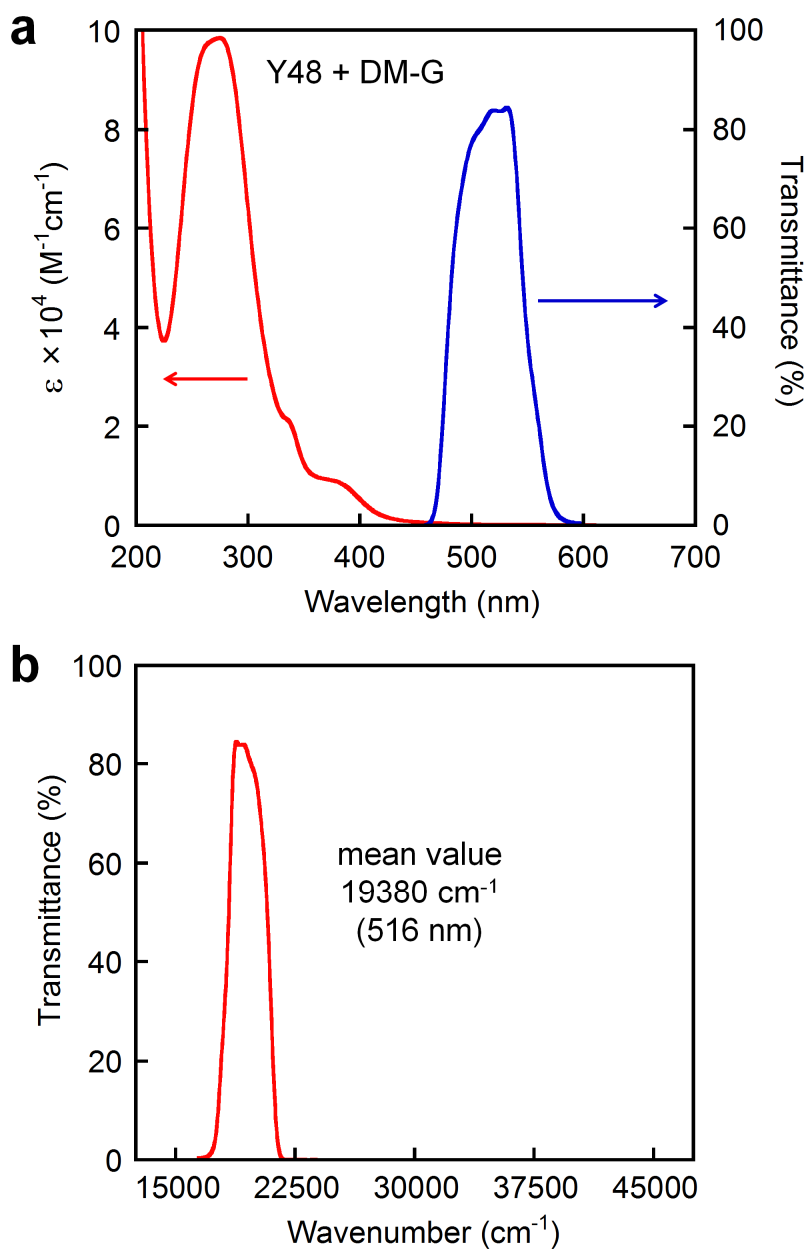


**Figure S21.** (a) Transmission spectrum for a set of interference filters Y48 + DM-G (blue line), and the molar absorptivity ( $\epsilon$ ) spectrum of  $[\text{PtCl}_2(\text{dpbpyMV4})](\text{PF}_6)_8$  in a 0.1 M NaCl aqueous solution at 20 °C in air (red line). (b) Transmission spectrum for a set of interference filters Y48 + DM-G as a function of wavenumber, which was used to determine the mean value for the light energy.

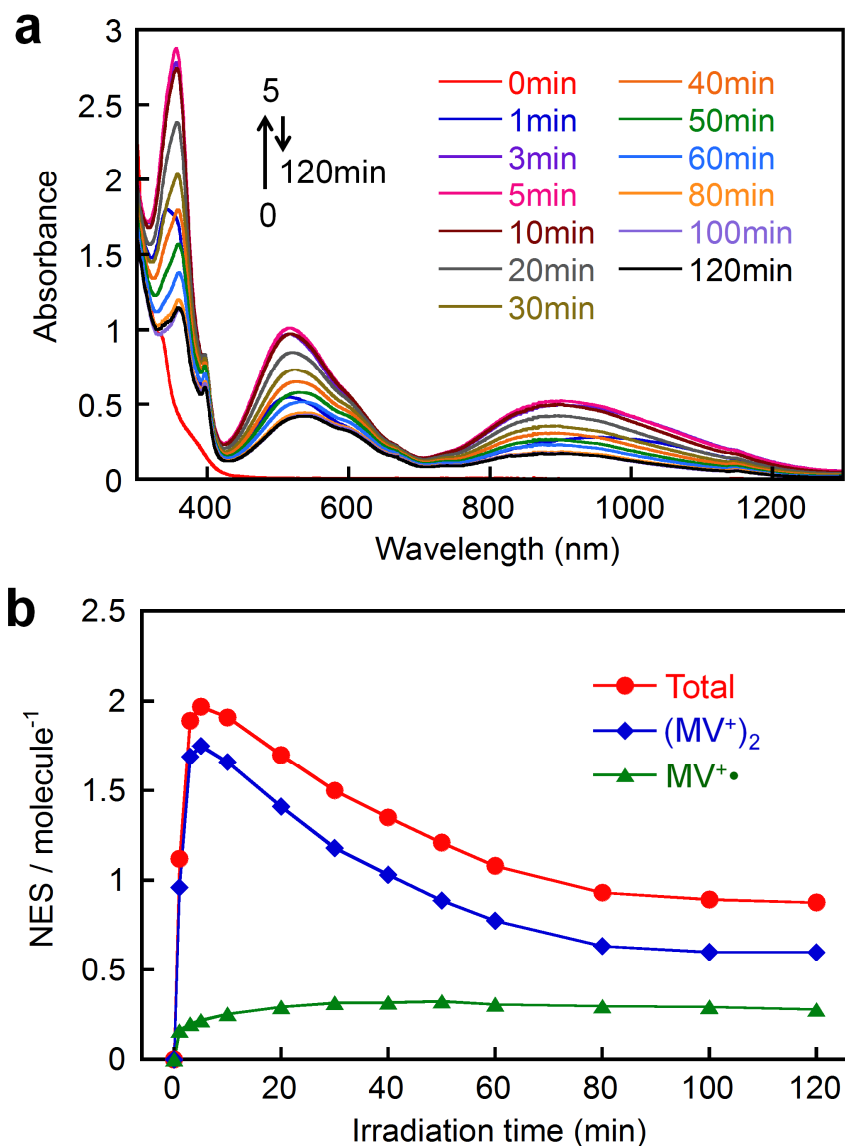


**Figure S22.** (a) Spectral changes during the photolysis of an aqueous acetate buffer solution (0.03 M CH<sub>3</sub>COOH and 0.07 M CH<sub>3</sub>COONa; pH 5.0, at 20 °C under Ar) containing 30 mM EDTA in the presence of 0.05 mM [PtCl<sub>2</sub>(d**pbpy**MV4)]Cl<sub>8</sub>. (b) The time course of the total NES together with those derived from the individual MV<sup>+</sup>• and (MV<sup>+</sup>)<sub>2</sub> components.

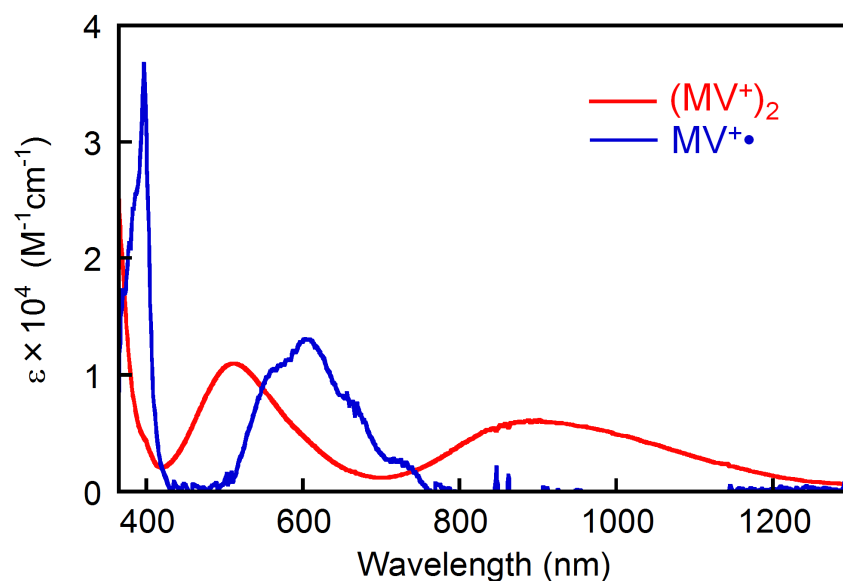


**Figure S23.** The two spectral components, corresponding to  $MV^{+\bullet}$  and  $(MV^+)_2$  generated over  $[PtCl_2(dpbpyMV4)]Cl_8$ , given by deconvolution of the data in Figure S22.

**Table S4.** Molar absorptivities determined for  $MV^{+\bullet}$  and  $(MV^+)_2$  generated over  $[PtCl_2(dpbpyMV4)]Cl_8$ , where the values are taken from those in Figure S23.

Species	$\lambda_{\text{abs}} / \text{nm}$	$\epsilon / \text{M}^{-1}\text{cm}^{-1}$
$(MV^+)_2$	354	29 000
	514	11 000
	889	6 100
$MV^{+\bullet}$	397	36 700
	603	13 100

**Table S5.** The net concentrations of  $MV^{+\bullet}$  and  $(MV^+)_2$  during the photolysis of  $[PtCl_2(dpbbpyMV4)]Cl_8$  together with some relevant parameters.

Irradiation time / min	Concentration / M		Abundance / %		$N_{total}^a$ / molecule <sup>-1</sup>	$K_d / M^{-1b}$
	$(MV^+)_2$	$MV^{+\bullet}$	$(MV^+)_2$	$MV^{+\bullet}$		
1	$2.40 \times 10^{-5}$	$8.01 \times 10^{-6}$	24.0	4.00	1.12	$3.74 \times 10^5$
3	$4.23 \times 10^{-5}$	$9.91 \times 10^{-6}$	42.3	4.96	1.89	$4.31 \times 10^5$
5	$4.38 \times 10^{-5}$	$1.08 \times 10^{-5}$	43.8	5.42	1.97	$3.73 \times 10^5$
10	$4.14 \times 10^{-5}$	$1.27 \times 10^{-5}$	41.4	6.35	1.91	$2.57 \times 10^5$
20	$3.53 \times 10^{-5}$	$1.46 \times 10^{-5}$	35.3	7.31	1.70	$1.65 \times 10^5$
30	$2.96 \times 10^{-5}$	$1.57 \times 10^{-5}$	29.6	7.85	1.50	$1.20 \times 10^5$
40	$2.58 \times 10^{-5}$	$1.59 \times 10^{-5}$	25.8	7.93	1.35	$1.03 \times 10^5$
50	$2.22 \times 10^{-5}$	$1.62 \times 10^{-5}$	22.2	8.10	1.21	$8.46 \times 10^4$
60	$1.94 \times 10^{-5}$	$1.53 \times 10^{-5}$	19.4	7.67	1.08	$8.22 \times 10^4$
80	$1.58 \times 10^{-5}$	$1.49 \times 10^{-5}$	15.8	7.43	0.93	$7.18 \times 10^4$
100	$1.50 \times 10^{-5}$	$1.47 \times 10^{-5}$	15.0	7.34	0.90	$6.97 \times 10^4$
120	$1.50 \times 10^{-5}$	$1.39 \times 10^{-5}$	15.0	6.96	0.88	$7.74 \times 10^4$

<sup>a</sup>The number of electron charged per molecule. <sup>b</sup>The apparent dimerization constant;  $K_d = [D][M]^{-2}$ .

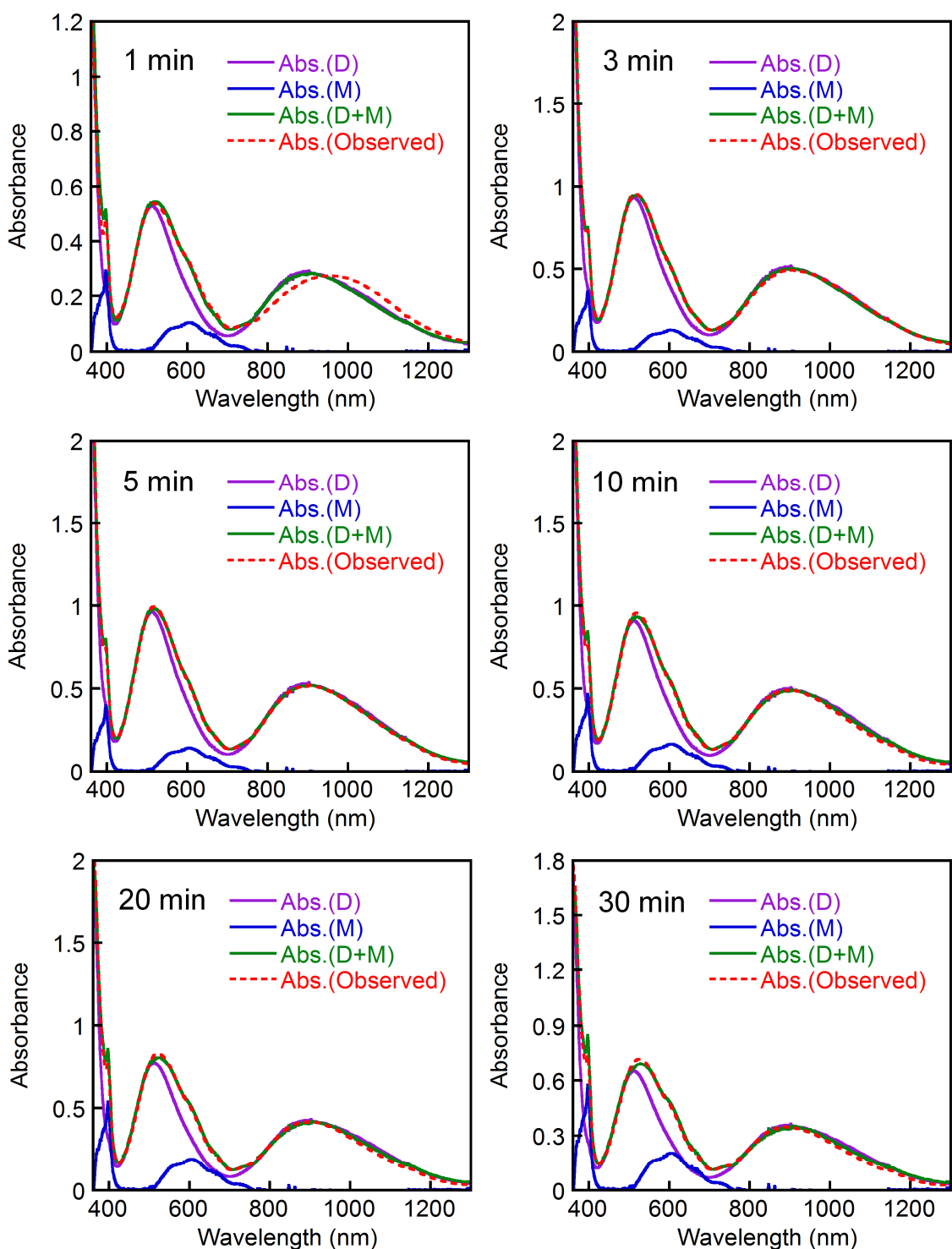


**Figure S24.** Deconvolution of the spectral data observed during the photolysis of  $[\text{PtCl}_2(\text{dpbpyMV4})]\text{Cl}_8$ , where the raw data are those in Figure S22. Each spectrum was fitted to the sum of two spectral components shown in Figure S23, where the concentrations of  $\text{MV}^{\bullet+}$  and  $(\text{MV}^+)_2$  were determined by the least-squares method implemented in our program.

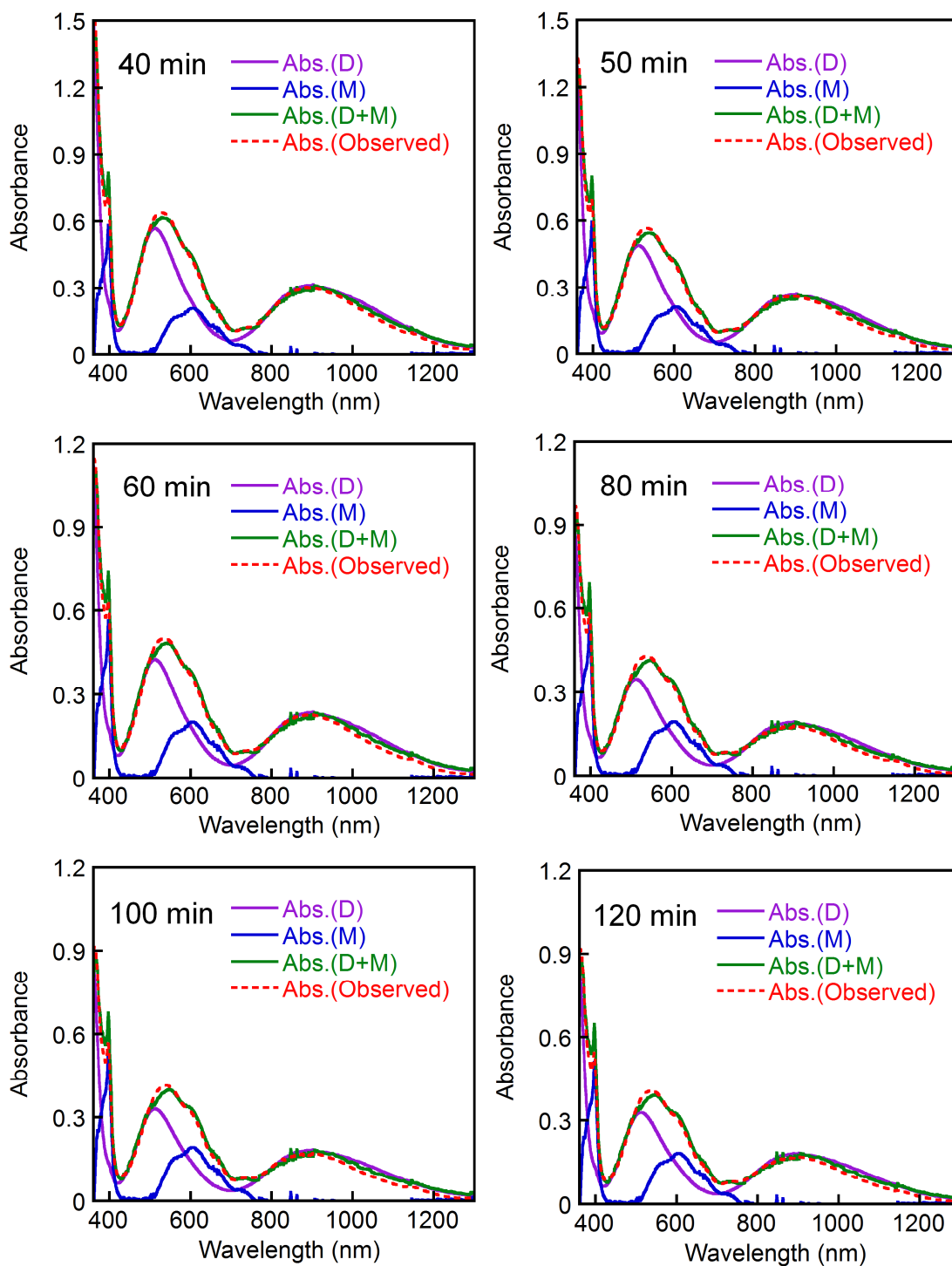
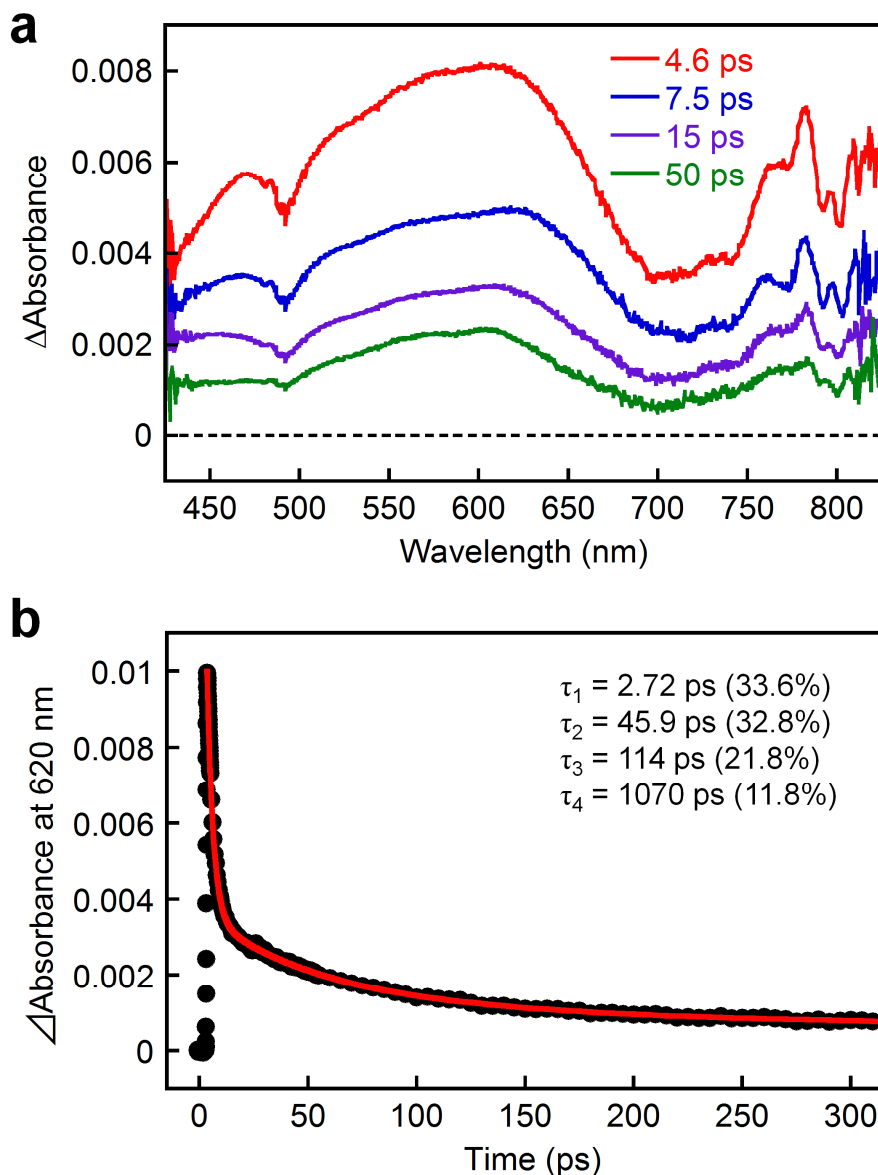
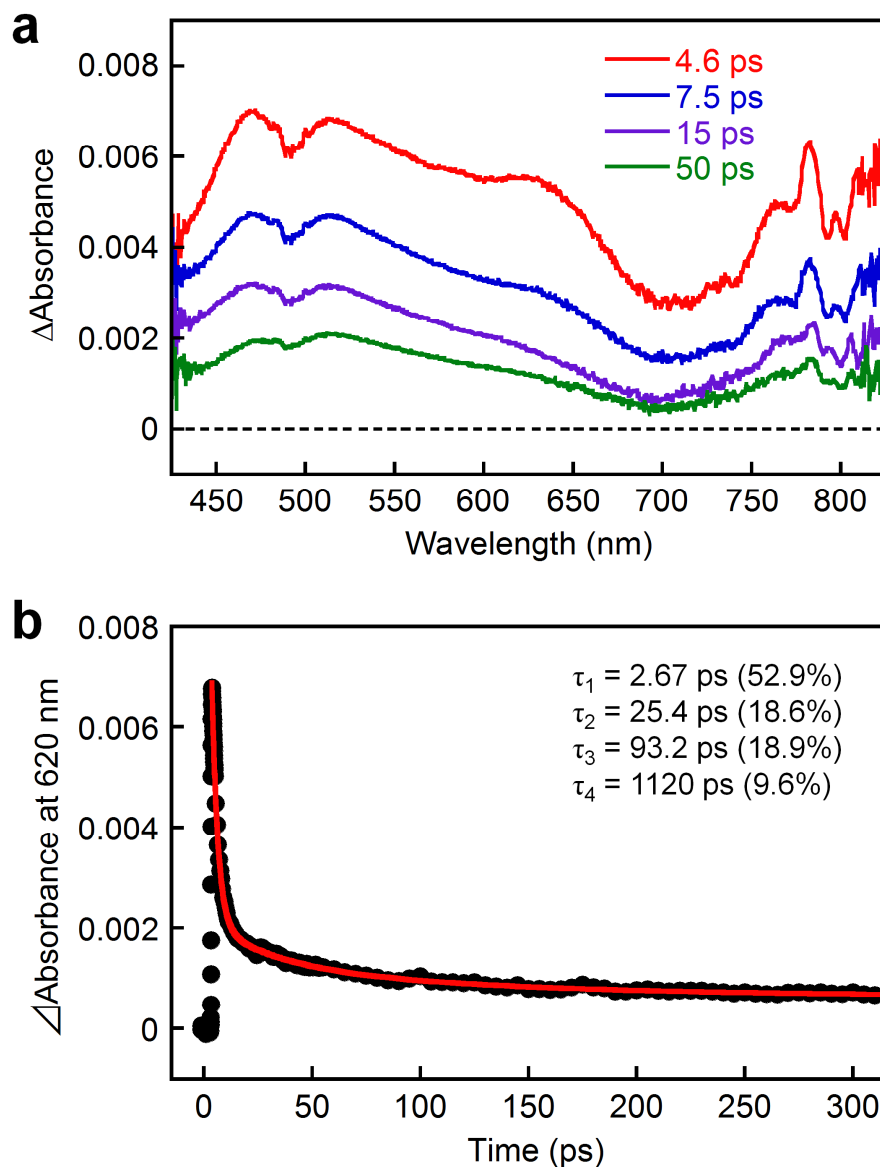


Figure S24 (Continued).



**Figure S25.** (a) Picosecond transient absorption spectra observed for an acetonitrile solution containing 1 mM  $[\text{PtCl}_2(\text{dpbpyMV4})](\text{PF}_6)_8$  under  $\text{N}_2$  atmosphere at room temperature, recorded after pulsing the 400-nm pump source. (b) Transient decay in absorption at 620 nm, where the red line corresponds to a calculated line based on a least-squares fit to a quadruple exponential function.



**Figure S26.** (a) Picosecond transient absorption spectra observed for an acetonitrile solution containing 1 mM  $\text{PtCl}_2(\text{dpbpyOBzl})$  under  $\text{N}_2$  atmosphere at room temperature, recorded after pulsing the 400-nm pump source. (b) Transient decay in absorption at 620 nm, where the red line corresponds to a calculated line based on a least-squares fit to a quadruple exponential function.

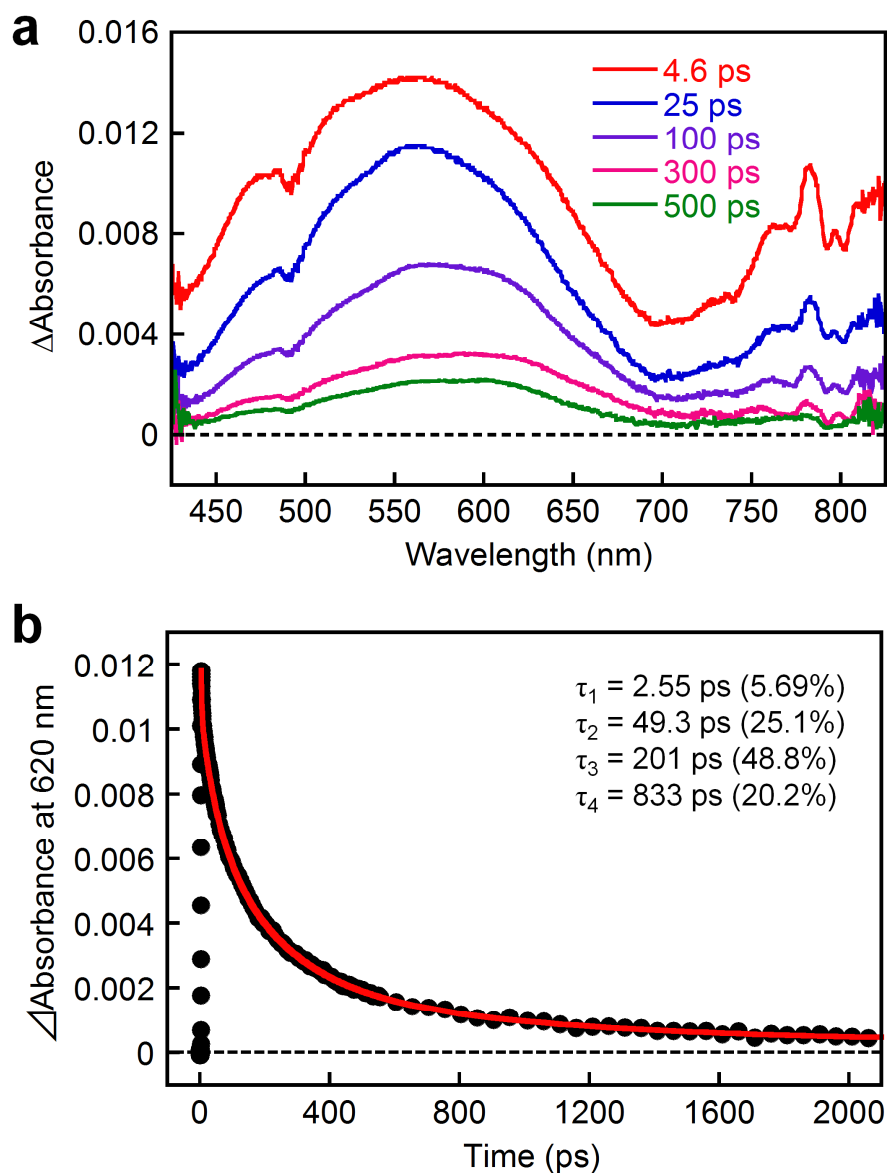


**Figure S27.** (a) Picosecond transient absorption spectra observed for an aqueous acetate buffer solution (0.03 M CH<sub>3</sub>COOH and 0.07 M CH<sub>3</sub>COONa; pH 5.0, at 20 °C under Ar) containing 1 mM [PtCl<sub>2</sub>(d**pbpy**MV4)](Cl)<sub>8</sub> and 0.1 M NaCl in the absence of EDTA under N<sub>2</sub> atmosphere at room temperature, recorded after pulsing the 400-nm pump source. (b) Transient decay in absorption at 620 nm, where the red line corresponds to a calculated line based on a least-squares fit to a quadruple exponential function.

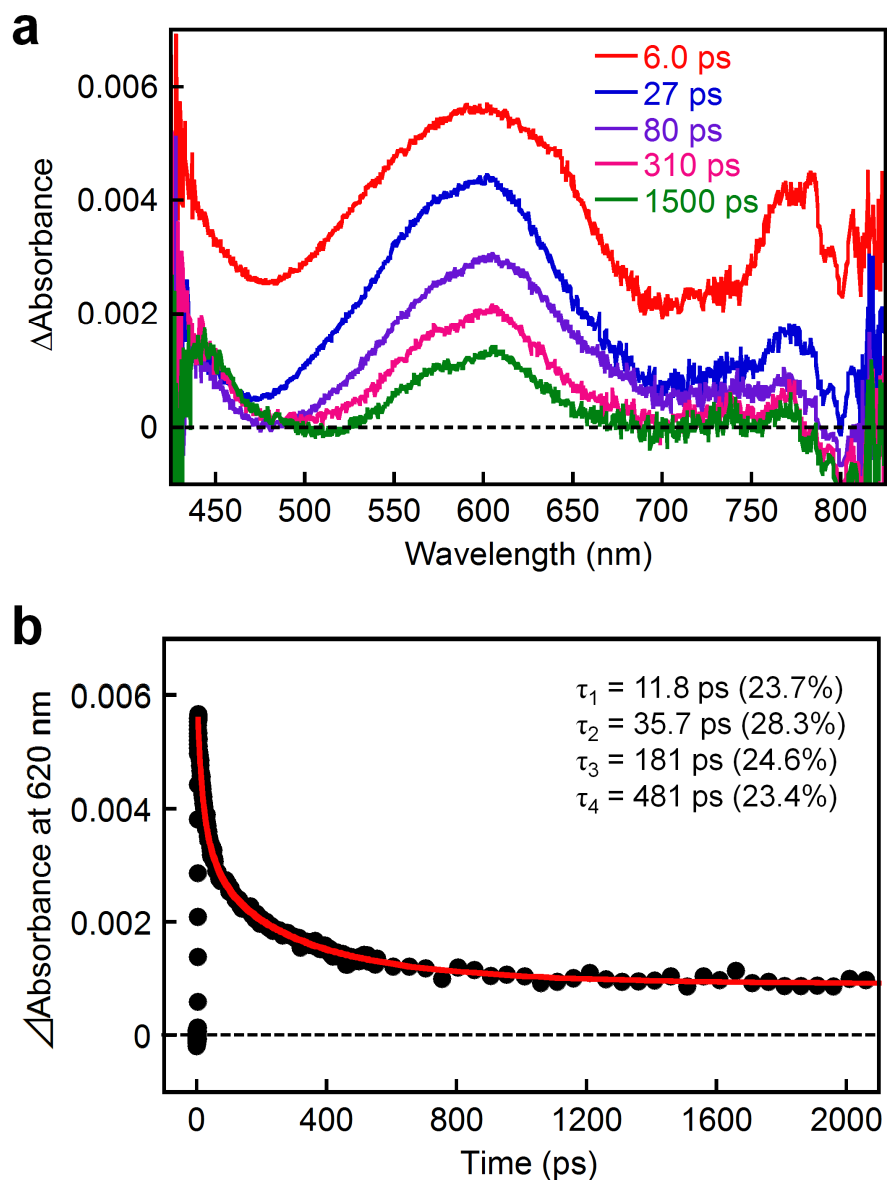


**Figure S28.** (a) Picosecond transient absorption spectra observed for an aqueous acetate buffer solution (0.03 M CH<sub>3</sub>COOH and 0.07 M CH<sub>3</sub>COONa; pH 5.0, at 20 °C under Ar) containing 1 mM [PtCl<sub>2</sub>(dppyMV4)](Cl)<sub>8</sub> and 0.1 M NaCl in the presence of 30 mM EDTA under N<sub>2</sub> atmosphere at room temperature, recorded after pulsing the 400-nm pump source. (b) Transient decay in absorption at 620 nm, where the red line corresponds to a calculated line based on a least-squares fit to a quadruple exponential function.

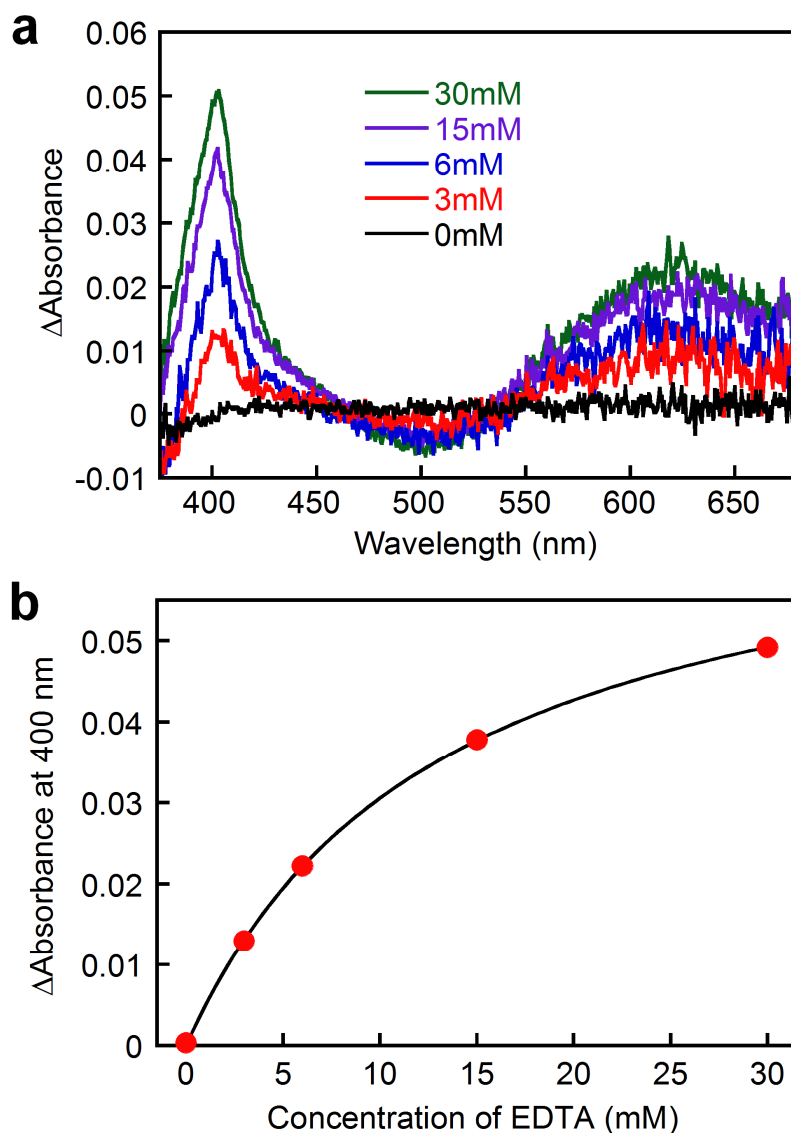


**Figure S29.** (a) Nanosecond transient absorption spectra observed for an aqueous acetate buffer solution (0.03 M  $\text{CH}_3\text{COOH}$  and 0.07 M  $\text{CH}_3\text{COONa}$ ; pH 5.0, at 20 °C under Ar) containing 0.1 mM  $[\text{PtCl}_2(\text{dpbpyMV4})(\text{PF}_6)_8]$  and 0.1 M NaCl in the presence of EDTA at various concentrations (0–30 mM), recorded at 50 ns after laser pulse excitation at 355 nm. (b) The dependence of the absorbance at 400 nm on the EDTA concentration (0–30 mM).

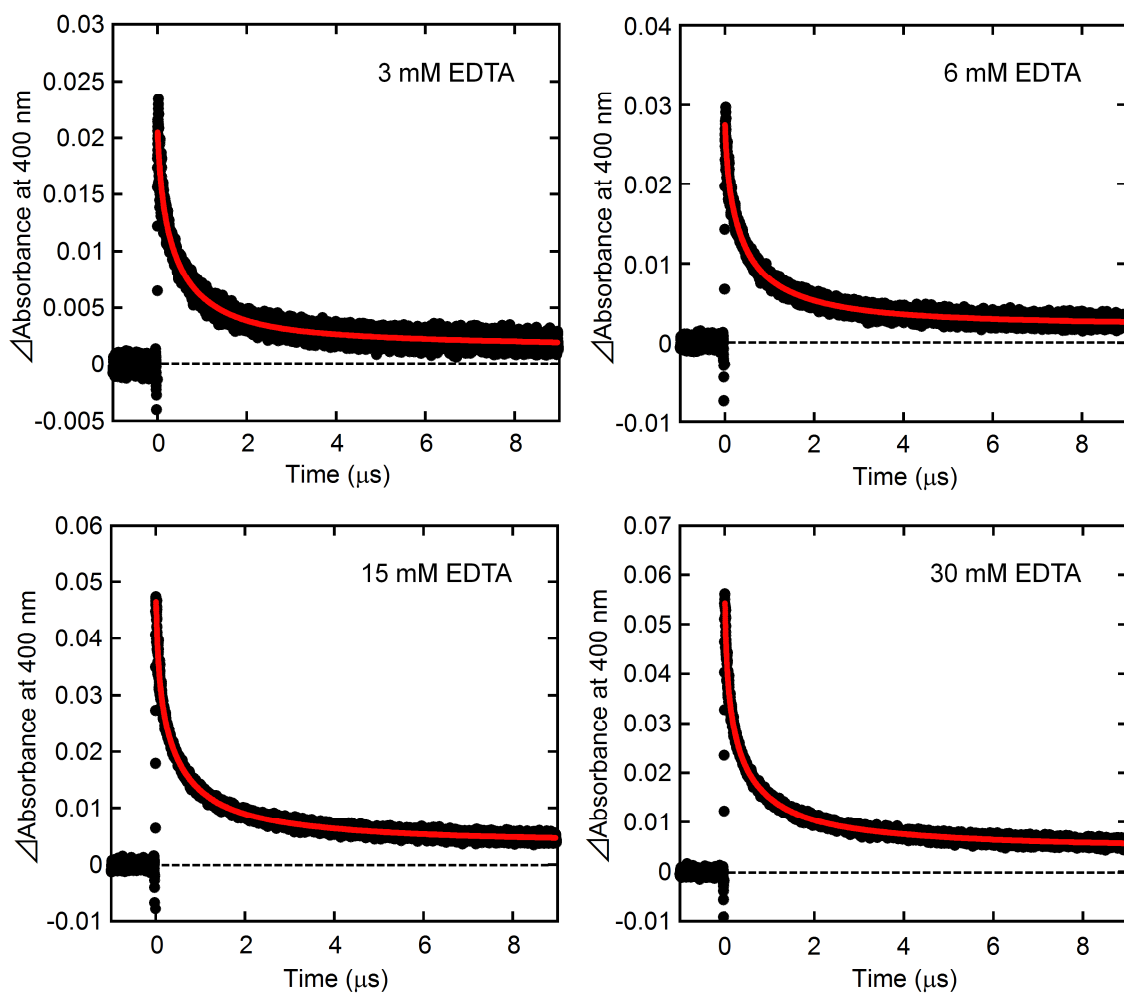


**Figure S30.** Nanosecond transient absorption changes at 400 nm observed for an aqueous acetate buffer solution (0.03 M  $\text{CH}_3\text{COOH}$  and 0.07 M  $\text{CH}_3\text{COONa}$ ; pH 5.0, at 20 °C under Ar) containing 0.1 mM  $[\text{PtCl}_2(\text{dpbpyMV4})(\text{PF}_6)_8]$  and 0.1 M NaCl in the presence of EDTA at various concentrations (3–30 mM), recorded after laser pulse excitation at 355 nm. The red line corresponds to a calculated line based on a least-squares fit to a quadruple exponential function.

**Table S6.** Lifetimes given in the least-squares fitting of the nanosecond transient absorption decays at 400 nm in the presence of EDTA (3–30 mM).

EDTA / mM	Lifetime	Relative contribution	Recombination ratio
3	$\tau_1 = 60.0$ ns	$\chi_1 = 17.1$ %	92 %
	$\tau_2 = 228$ ns	$\chi_2 = 28.4$ %	
	$\tau_3 = 827$ ns	$\chi_3 = 41.8$ %	
	$\tau_4 = 4.06$ $\mu$ s	$\chi_4 = 12.7$ %	
6	$\tau_1 = 52.3$ ns	$\chi_1 = 20.7$ %	92 %
	$\tau_2 = 296$ ns	$\chi_2 = 35.7$ %	
	$\tau_3 = 1.05$ $\mu$ s	$\chi_3 = 31.6$ %	
	$\tau_4 = 3.79$ $\mu$ s	$\chi_4 = 12.0$ %	
15	$\tau_1 = 35.8$ ns	$\chi_1 = 20.5$ %	91 %
	$\tau_2 = 148$ ns	$\chi_2 = 25.2$ %	
	$\tau_3 = 615$ ns	$\chi_3 = 36.1$ %	
	$\tau_4 = 2.87$ $\mu$ s	$\chi_4 = 18.2$ %	
30	$\tau_1 = 30.8$ ns	$\chi_1 = 23.8$ %	91 %
	$\tau_2 = 161$ ns	$\chi_2 = 28.4$ %	
	$\tau_3 = 683$ ns	$\chi_3 = 32.2$ %	
	$\tau_4 = 3.18$ $\mu$ s	$\chi_4 = 15.6$ %	

## References

- [S1] N. R. Kelly, S. Goetz, C. S. Hawes and P. E. Kruger, *Tetrahedron Lett.*, 2011, **52**, 995.  
[S2] L. A. Kelly and M. A. J. Rodgers, *J. Phys. Chem.*, 1994, **98**, 6386.  
[S3] J. H. Price, A. N. Williamson, R. F. Schramm and B. B. Wayland, *Inorg. Chem.*, 1972, **11**, 1280.  
[S4] K. Kitamoto and K. Sakai, *Angew. Chem. Int. Ed.*, 2014, **53**, 4618.  
[S5] M. Kobayashi, S. Masaoka and K. Sakai, *Dalton Trans.* 2012, **41**, 4903.